Supplementary material 1 - Discntinuous Epitope Predictions from Molecular Dynamics Outputs

Carlos Francisco Sampaio Bonafé (in memoriam)[1] Juan Philippe Teixeira[2]
Caio Cesar de Melo Freire[3] Miklos Maximiliano Bajay[2]
Daniel Ferreira de Lima Neto[2]

2026-05-31

Contents

Conformational Epitope Prediction

Conformational B-cell epitope prediction with DiscoTope is fundamentally a structure-based exercise that couples residue-level propensities with measures of surface exposure to infer discontinuous antigenic patches. The original method (DiscoTope 1.0) introduced the idea of combining 3D neighborhood information with amino-acid propensities derived from curated antigen–antibody complexes; DiscoTope 2.0 refined this by adopting an improved surface metric (half-sphere exposure), revised spatial neighborhoods, and re-benchmarked thresholds, leading to more reliable performance across independent test sets. Mechanistically, DiscoTope flags residues that are simultaneously (i) enriched for epitope-favored chemistries and (ii) sufficiently accessible on the native fold—features that map well onto the known enrichment of conformational epitopes in flexible, solvent-exposed loops and protrusions. These modeling choices are well documented in the method's primary papers and the DTU server description, and they align with broader reviews showing that accessibility and local dynamics are the strongest single-feature correlates of epitope location.

A central variable in that framework is relative solvent accessibility (RSA)—a normalized expression of solvent-accessible surface area (SASA)—which is typically calculated using Shrake–Rupley "rolling-probe" geometry. Because DiscoTope's scoring depends on surface exposure, any perturbation that shifts the protein's solvent-exposed landscape will alter predicted epitope patches. High pressure is exactly such a perturbation: it favors conformations with reduced system volume (protein + solvent), thereby encouraging

the collapse of internal cavities, water penetration into hydrophobic cores, and redistribution of hydrogen-bond/salt-bridge networks. NMR/crystallographic and simulation studies show that pressure-driven unfolding or partial unfolding is often initiated at pre-existing voids and flexible segments, which can change RSA in a residue-specific manner—precisely the type of signal DiscoTope reads. Thus, as hydrostatic pressure increases, one expects non-monotonic RSA changes across the surface: modest pressures unmask cryptic but native-adjacent patches; higher pressures promote larger rearrangements that create entirely new non-native antigenic surfaces. This picture is well supported by the protein-under-pressure literature on cavity collapse and hydration, and by quantitative analyses linking unfolding volume changes to internal voids.

TMV provides a well-characterized testbed for these ideas. Structurally, TMV is a helical nucleoprotein rod composed of ~2,130 copies of a 158-residue coat protein wrapped around a single-stranded RNA; decades of fiber diffraction and, more recently, high-resolution cryo-EM have established atomic models for both the intact virion and assembly intermediates. This precise structural knowledge is ideal for surface-based epitope prediction and for modeling pressure responses, because it anchors RSA estimates to a realistic 3D framework. In practical terms, DiscoTope run on atomistic TMV models will report different epitope landscapes as pressure shifts loop flexibilities, side-chain rotamers, and inter-subunit contacts that define the solvent-exposed helical grooves and lateral interfaces.

Experimentally, these expectations were borne out in the TMV literature: exposure to HHP altered the pattern of antibody recognition relative to native virions, with moderate pressures revealing previously masked epitopes and higher pressures enabling recognition of neo-exposed patches. In the Virology Journal study by Ferreira de Lima Neto and Bonafé, pressure (alone and in combination with low temperature or urea) reshaped the serological fingerprint of TMV, consistent with a hierarchical destabilization of structural domains under pressure and a graded unmasking of antigenic sites. The concordance between (i) the direction and residue-level logic of RSA changes predicted by structure-based tools and (ii) the experimental epitope mapping across pressure conditions validates the conceptual bridge between DiscoTope outputs and pressure-modulated antigenicity.

At the level of physical chemistry, the pressure dependence of protein conformations naturally extends to antibody–antigen complexes: pressures in the 1–4 kbar range can reversibly dissociate oligomers and even some antigen–antibody pairs, reflecting positive volume changes of association. This thermodynamic lens helps interpret pressure-dependent serological assays and suggests that certain antibody interactions will be more pressure-labile than others, depending on interfacial packing, trapped solvent, and cavity formation upon binding. When such complexes dissociate under pressure, epitope exposure measured on the free antigen may no longer mirror the epitope as presented in the bound state—an important caveat that encourages combining DiscoTope with explicit modeling of binding interfaces and, where possible, wet-lab pressure perturbations in sera or monoclonals.

Mechanistically, several linked processes coherently explain the stepwise changes we observe in TMV under pressure and their readout by DiscoTope. First, small increases in pressure perturb marginal tertiary contacts and side-chain packing, often at pre-existing surface grooves or inter-subunit seams, causing local RSA increases without wholesale unfolding; DiscoTope registers these as strengthened or expanded patches around native-adjacent epitopes. Second, further pressure drives water into shallow cavities and along hydrogen-bond networks, increasing local compressibility and micro-hydration; flexible loops and termini become more dynamic, sometimes flipping out to expose new surfaces that score as epitopes. Third, at still higher pressure, partial unfolding or inter-subunit slippage modifies the helical lattice, generating non-native protrusions and de-novo patches that only become DiscoTope-positive in these states. The literature on pressure-induced cavity collapse, hydration, and the primacy of voids in pressure unfolding supports each link of this cascade.

This HHP-tunable antigenic landscape has practical consequences. For discovery, pressure acts as a controlled perturbation to reveal cryptic epitopes—regions immunologically silent at ambient conditions yet structurally predisposed to exposure. For engineering, pressure-responsive "weak points" can be mapped and then stabilized or destabilized (e.g., by targeted mutations or formulation) to bias epitope display in vaccines or diagnostics. For analytical virology, pairing DiscoTope (or related structure-based tools such as ElliPro/SEPPA) with pressure series and RSA tracking offers a quantitative route to rank epitope robustness across environmental stresses relevant to processing, inactivation, or storage. The broader HHP

virology literature—though focused mostly on foodborne pathogens—reinforces that capsid proteins are pressure-sensitive in ways that change exposure and immunoreactivity, mirroring what is observed in TMV at the structural/epitope level.

Placing these observations in a methodological context, it is worth recalling both the strengths and limits of structure-based epitope predictors. DiscoTope's reliance on 3D structure and exposure metrics offers specificity for conformational epitopes, outperforming single-feature scales that track only hydrophilicity or flexibility. Yet no single predictor captures the full immunogenic reality: bound vs. unbound conformations, quaternary arrangements, glycosylation or ion occupancy (e.g., Ca^2 effects in TMV assemblies), and pressure-coupled dynamics can all modulate the true paratope–epitope interface. Hence, convergent evidence—structure-based predictions under multiple conditions, complementary tools, and experimental mapping—provides the most reliable guide for identifying pressure-sensitive antigenic sites.

Structural Models and Epitope Prediction

Protein structures were obtained in PDB format from molecular dynamics trajectories and used as input for conformational B-cell epitope prediction. Conformational epitopes were identified with DiscoTope 3.0, which provides per-residue prediction scores calibrated to surface exposure and residue statistics. The output was tabulated in .csv files, containing residue identity, position, chain information, DiscoTope score, calibrated score, epitope classification, relative solvent accessibility (RSA), and confidence values (pLDDT).

Mapping of Epitope Scores to B-Factors

To enable three-dimensional visualization, DiscoTope scores were programmatically mapped to the B-factor field of the corresponding PDB coordinate files. A custom Python script was developed to (i) parse .csv outputs, (ii) match residues to their structural counterparts in the PDB, and (iii) overwrite the B-factor field with normalized DiscoTope values. Only residues present in both the prediction table and the structural file were annotated. This approach allowed downstream molecular viewers to interpret epitope propensities as temperature-factor–like values without altering the structural coordinates.

PyMOL Visualization and Selective Coloring

Visualization and figure preparation were performed using PyMOL 2.0. All structures were initially rendered in cartoon representation and colored uniformly in light gray to emphasize highlighted regions. Residues with DiscoTope scores below 0.35 were displayed using a blue–white–red gradient proportional to their score distribution. Residues with scores 0.35, considered higher-confidence epitope candidates, were isolated as a separate selection and colored using a yellow–orange–red ramp, with increasing intensity reflecting higher scores. Non-epitope regions were partially transparent to improve visual contrast. Epitope residues were also displayed as spheres to facilitate identification.

Automated Figure Generation

To standardize figure production across multiple experimental conditions, a PyMOL automation pipeline was implemented. For each PDB annotated with epitope scores, a .pml script was generated that loaded the structure, applied the color ramps, oriented the view, and exported publication-quality images (.png). For each object, two views were systematically generated: a front orientation and a 180° rotation along the Z-axis, saved at 2000×2000 pixels with ray tracing enabled. Outputs were stored in a structured directory (figs/) with filenames encoding experimental identifiers.

Comparative Visualization in R Markdown

Processed images were integrated into a reproducible R Markdown workflow. Using the cowplot package in R, images corresponding to different pressure–temperature conditions were assembled into multi-panel figures (plot_grid). Each panel was annotated with the corresponding condition (e.g., "A) 1 bar", "B) 250 bar") using draw_label. Figures were arranged in two-column layouts for balanced comparison, with residual

plots centered when odd numbers of panels were present. This ensured consistency and comparability across up to 21 independent conditions.

Data Analysis and Statistical Evaluation

In parallel to structural visualization, DiscoTope scores and associated residue-level metrics were analyzed using Python (pandas, NumPy, SciPy, Matplotlib). For each experiment, the correlation between DiscoTope scores and relative solvent accessibility (RSA) was calculated using Pearson's correlation coefficient. This step provided an internal validation of whether epitope prediction was influenced by solvent exposure. In addition, distributions of DiscoTope scores were evaluated by plotting histograms, cumulative frequency plots, and boxplots, allowing the identification of threshold-dependent subsets of residues. Comparisons across experimental conditions (e.g., pressure or temperature series) were made by aggregating CSV results and calculating summary statistics per replicate (mean, median, interquartile range). Outliers were detected by Tukey's rule and retained for visualization, as they may correspond to structurally relevant epitope hot-spots. Statistical outputs were saved in tabular .csv form and linked to the graphical representations. By combining quantitative statistical analysis of DiscoTope predictions with three-dimensional mapping and side-by-side figure layouts, the methodology ensured both numerical rigor and visual interpretability of predicted epitope landscapes under different biophysical conditions.

Discontinuous Epitope predicitons

HHP

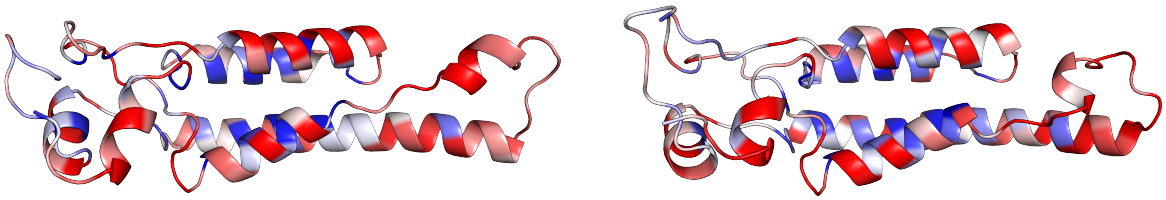

Figure 1: Epitope Preditions side-by-side - High Hydrostatic Pressure

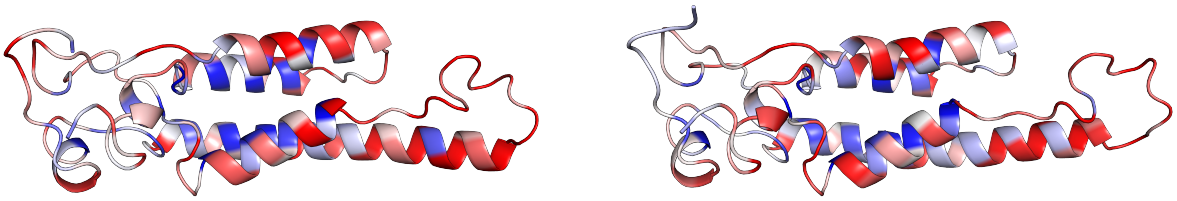

C) 500 bar D) 750 bar

Figure 2: Epitope Preditions side-by-side - High Hydrostatic Pressure

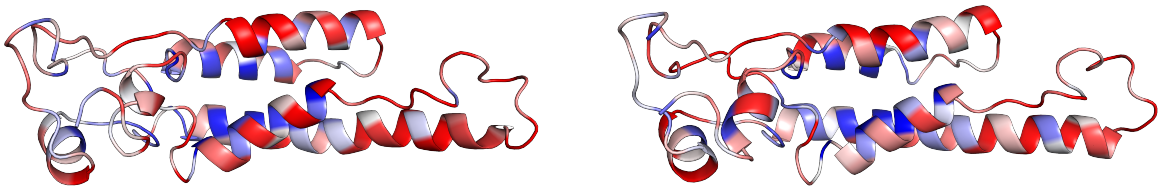

E) 1000 bar F) 1250 bar

Figure 3: Epitope Preditions side-by-side - High Hydrostatic Pressure

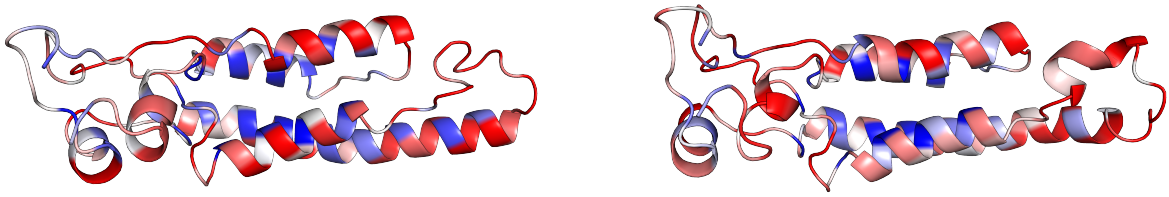

G) 1500 bar H) 1750 bar

Figure 4: Epitope Preditions side-by-side - High Hydrostatic Pressure

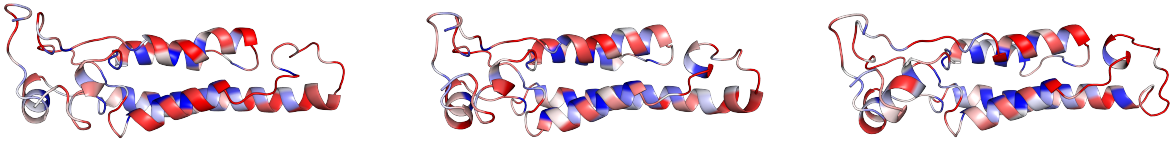

I) 2000 bar J) 2250 bar K) 2500 bar

Figure 5: Epitope Preditions side-by-side - High Hydrostatic Pressure

HHP and low temperature

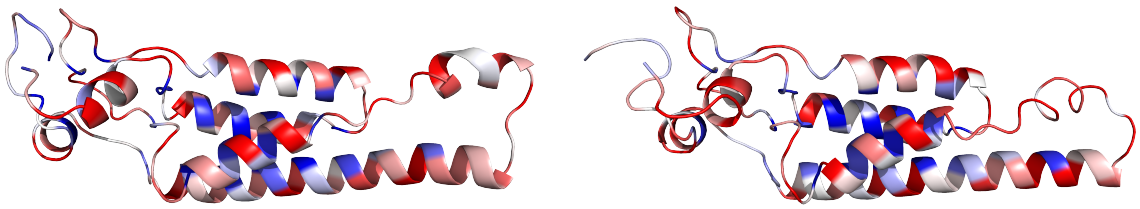

A) 1 bar B) 250 bar

Figure 6: Epitope Preditions side-by-side - High Hydrostatic Pressure and Low Temperature

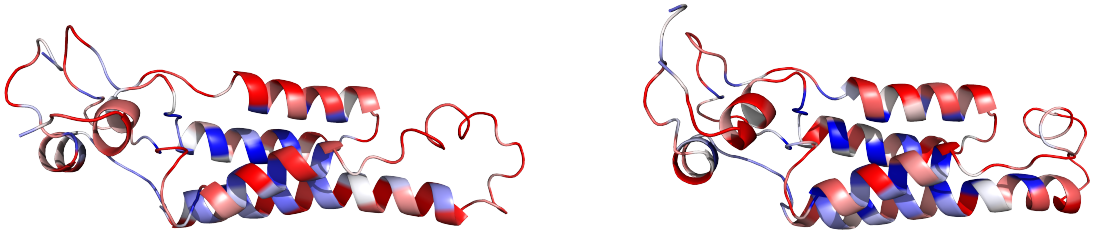

C) 500 bar D) 750 bar

Figure 7: Epitope Preditions side-by-side - High Hydrostatic Pressure and Low Temperature

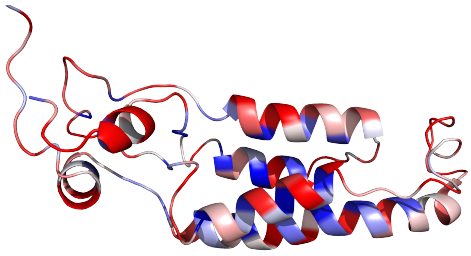

E) 1000 bar

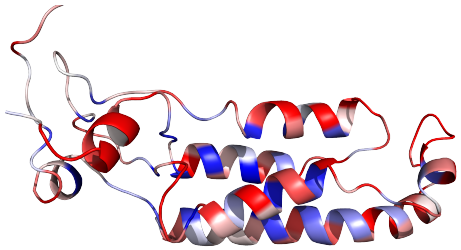

F) 1250 bar

Figure 8: Epitope Preditions side-by-side - High Hydrostatic Pressure and Low Temperature

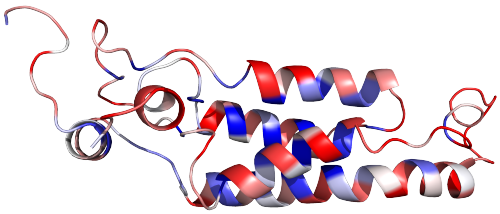

G) 1500 bar

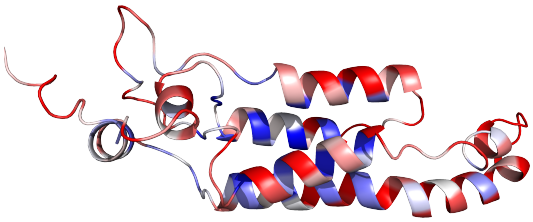

H) 1750 bar

Figure 9: Epitope Preditions side-by-side - High Hydrostatic Pressure and Low Temperature

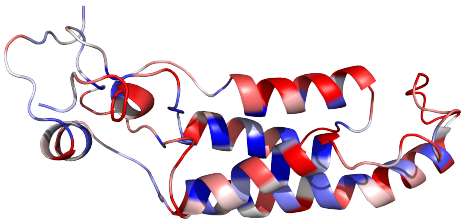

I) 2000 bar

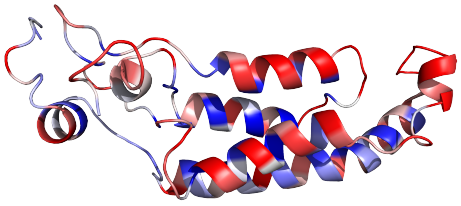

J) 2250 bar

Figure 10: Epitope Preditions side-by-side - High Hydrostatic Pressure and Low Temperature

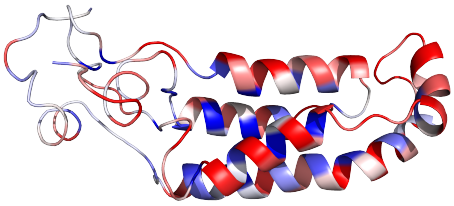

K) 2500 bar

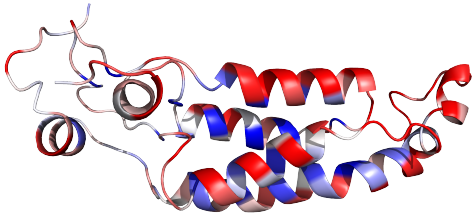

L) 2500 bar @ 300 k

Figure 11: Epitope Preditions side-by-side - High Hydrostatic Pressure and Low Temperature

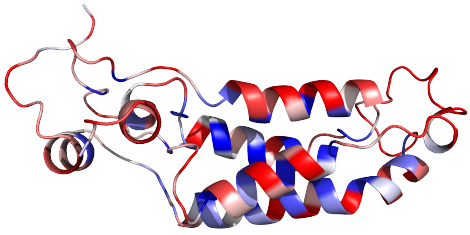

M) 2500 bar @ 295 k

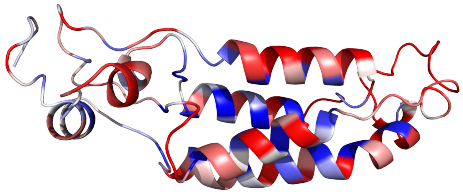

N) 2500 bar @ 290 k

Figure 12: Epitope Preditions side-by-side - High Hydrostatic Pressure and Low Temperature

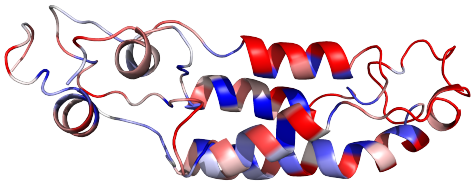

O) 2500 bar @ 285 k

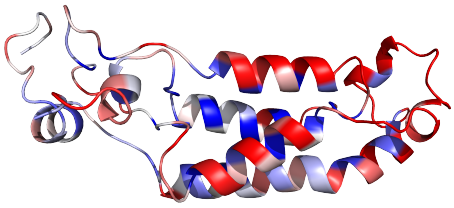

P) 2500 bar @ 280 k

Figure 13: Epitope Preditions side-by-side - High Hydrostatic Pressure and Low Temperature

Q) 2500 bar @ 275 k R) 2500 bar @ 270 k

Figure 14: Epitope Preditions side-by-side - High Hydrostatic Pressure and Low Temperature

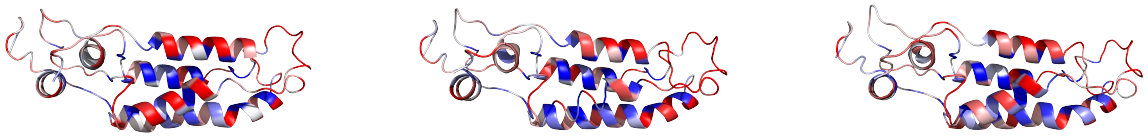

S) 2500 bar @ 265 k T) 2500 bar @ 260 k U) 2500 bar @ 255 k

Figure 15: Epitope Preditions side-by-side - High Hydrostatic Pressure and Low Temperature

Discotope tabular results

HHP

Residues with DiscoTope ≥ 0.35 — md_0_1_A_discotope3.csv (n = 17)

PDB	Chain	ResID	AA	DiscoTope	Calibrated	Epitope	RSA	pLDDT	Length	AF2 flag
md_0_1_A	A	92	R	0.52813	2.15947	TRUE	0.64816	100	155	0
md_0_1_A	A	46	R	0.50507	1.99032	TRUE	0.58819	100	155	0
md_0_1_A	A	72	Y	0.46701	1.71113	TRUE	0.42973	100	155	0
md_0_1_A	A	73	N	0.44853	1.57558	TRUE	0.14330	100	155	0
md_0_1_A	A	64	D	0.42569	1.40804	TRUE	0.64877	100	155	0
md_0_1_A	A	95	E	0.41221	1.30916	TRUE	0.74165	100	155	0
md_0_1_A	A	147	S	0.40082	1.22561	TRUE	0.58847	100	155	0
md_0_1_A	A	50	E	0.39528	1.18497	TRUE	0.69301	100	155	0
md_0_1_A	A	7	P	0.39110	1.15431	TRUE	0.80617	100	155	0
md_0_1_A	A	10	F	0.39020	1.14771	TRUE	0.59925	100	155	0
md_0_1_A	A	39	Q	0.38660	1.12130	TRUE	0.63616	100	155	0
md_0_1_A	A	91	N	0.38358	1.09915	TRUE	0.20280	100	155	0
md_0_1_A	A	53	K	0.38293	1.09438	TRUE	0.60781	100	155	0
md_0_1_A	A	90	R	0.37395	1.02851	TRUE	0.59534	100	155	0
md_0_1_A	A	42	T	0.37386	1.02785	TRUE	0.29709	100	155	0
md_0_1_A	A	54	P	0.36824	0.98662	TRUE	0.43247	100	155	0
md_0_1_A	A	74	A	0.35988	0.92530	TRUE	0.82693	100	155	0

Figure 16: Residues with DiscoTope above the threshold of 0.35 — md-0-1-A-discotope3.csv (n = 17)

Residues with DiscoTope ≥ 0.35 — md_0_2_A_discotope3.csv (n = 25)

PDB	Chain	ResID	AA	DiscoTope	Calibrated	Epitope	RSA	pLDDT	Length	AF2 flag
md_0_2_A	A	93	I	0.49887	1.94972	TRUE	0.59715	100	155	0
md_0_2_A	A	103	T	0.49848	1.94685	TRUE	0.45711	100	155	0
md_0_2_A	A	72	Y	0.48512	1.84860	TRUE	0.57653	100	155	0
md_0_2_A	A	108	L	0.43786	1.50107	TRUE	0.64370	100	155	0
md_0_2_A	A	91	N	0.41601	1.34039	TRUE	0.13431	100	155	0
md_0_2_A	A	102	P	0.41440	1.32855	TRUE	0.89200	100	155	0
md_0_2_A	A	99	Q	0.40570	1.26457	TRUE	0.95334	100	155	0
md_0_2_A	A	90	R	0.40470	1.25722	TRUE	0.45870	100	155	0
md_0_2_A	A	104	T	0.39450	1.18221	TRUE	0.79505	100	155	0
md_0_2_A	A	77	D	0.38887	1.14081	TRUE	0.26426	100	155	0
md_0_2_A	A	81	T	0.38678	1.12544	TRUE	0.53012	100	155	0
md_0_2_A	A	109	D	0.38597	1.11948	TRUE	0.44171	100	155	0
md_0_2_A	A	100	A	0.38490	1.11161	TRUE	0.70926	100	155	0
md_0_2_A	A	15	S	0.37806	1.06131	TRUE	0.52621	100	155	0
md_0_2_A	A	112	R	0.37502	1.03896	TRUE	0.69976	100	155	0
md_0_2_A	A	92	R	0.37326	1.02602	TRUE	0.81143	100	155	0
md_0_2_A	A	74	A	0.37145	1.01271	TRUE	0.80167	100	155	0
md_0_2_A	A	126	N	0.36862	0.99189	TRUE	0.56531	100	155	0
md_0_2_A	A	46	R	0.36593	0.97211	TRUE	0.61600	100	155	0
md_0_2_A	A	123	S	0.35919	0.92255	TRUE	0.45534	100	155	0
md_0_2_A	A	39	Q	0.35885	0.92005	TRUE	0.69155	100	155	0
md_0_2_A	A	31	L	0.35714	0.90747	TRUE	0.35853	100	155	0
md_0_2_A	A	37	T	0.35476	0.88997	FALSE	0.63131	100	155	0
md_0_2_A	A	8	S	0.35377	0.88269	FALSE	0.52364	100	155	0
md_0_2_A	A	143	S	0.35357	0.88122	FALSE	0.36643	100	155	0

Figure 17: Residues with DiscoTope above the threshold of 0.35 — md-0-2-A-discotope3.csv (n = 25)

Residues with DiscoTope ≥ 0.35 — md_0_3_A_discotope3.csv (n = 23)

PDB	Chain	ResID	AA	DiscoTope	Calibrated	Epitope	RSA	pLDDT	Length	AF2 flag
md_0_3_A	A	112	R	0.53664	2.15527	TRUE	0.76469	100	155	0
md_0_3_A	A	99	Q	0.52612	2.08042	TRUE	0.81277	100	155	0
md_0_3_A	A	46	R	0.46022	1.61152	TRUE	0.60281	100	155	0
md_0_3_A	A	93	I	0.45997	1.60974	TRUE	0.88079	100	155	0
md_0_3_A	A	111	T	0.44858	1.52869	TRUE	0.48502	100	155	0
md_0_3_A	A	72	Y	0.41166	1.26599	TRUE	0.56827	100	155	0
md_0_3_A	A	92	R	0.40948	1.25048	TRUE	0.71155	100	155	0
md_0_3_A	A	96	V	0.39946	1.17919	TRUE	0.86230	100	155	0
md_0_3_A	A	97	E	0.39478	1.14589	TRUE	0.60762	100	155	0
md_0_3_A	A	109	D	0.39074	1.11714	TRUE	0.40563	100	155	0
md_0_3_A	A	102	P	0.38175	1.05317	TRUE	0.93103	100	155	0
md_0_3_A	A	122	R	0.37812	1.02734	TRUE	0.38897	100	155	0
md_0_3_A	A	115	D	0.37779	1.02499	TRUE	0.47676	100	155	0
md_0_3_A	A	91	N	0.37247	0.98714	TRUE	0.10493	100	155	0
md_0_3_A	A	88	D	0.37200	0.98380	TRUE	0.57465	100	155	0
md_0_3_A	A	123	S	0.36921	0.96394	TRUE	0.42498	100	155	0
md_0_3_A	A	108	L	0.36699	0.94815	TRUE	0.73677	100	155	0
md_0_3_A	A	134	R	0.36582	0.93982	TRUE	0.59791	100	155	0
md_0_3_A	A	54	P	0.36493	0.93349	TRUE	0.59188	100	155	0
md_0_3_A	A	29	N	0.36402	0.92702	TRUE	0.52502	100	155	0
md_0_3_A	A	33	N	0.35615	0.87102	FALSE	0.51885	100	155	0
md_0_3_A	A	105	A	0.35538	0.86554	FALSE	0.74988	100	155	0
md_0_3_A	A	103	T	0.35198	0.84135	FALSE	0.51201	100	155	0

Figure 18: Residues with DiscoTope above the threshold of 0.35 — md-0-3-A-discotope3.csv (n = 23)

Residues with DiscoTope ≥ 0.35 — md_0_4_A_discotope3.csv (n = 12)

PDB	Chain	ResID	AA	DiscoTope	Calibrated	Epitope	RSA	pLDDT	Length	AF2 flag
md_0_4_A	A	46	R	0.47236	1.87992	TRUE	0.48240	100	155	0
md_0_4_A	A	115	D	0.45979	1.78089	TRUE	0.53223	100	155	0
md_0_4_A	A	126	N	0.42662	1.51957	TRUE	0.57599	100	155	0
md_0_4_A	A	108	L	0.41829	1.45394	TRUE	0.61249	100	155	0
md_0_4_A	A	54	P	0.41426	1.42219	TRUE	0.68942	100	155	0
md_0_4_A	A	112	R	0.41224	1.40628	TRUE	0.60236	100	155	0
md_0_4_A	A	104	T	0.40393	1.34081	TRUE	0.99249	100	155	0
md_0_4_A	A	72	Y	0.40289	1.33262	TRUE	0.48711	100	155	0
md_0_4_A	A	99	Q	0.40059	1.31450	TRUE	0.86071	100	155	0
md_0_4_A	A	93	I	0.38341	1.17915	TRUE	0.67923	100	155	0
md_0_4_A	A	32	G	0.37094	1.08091	TRUE	0.76503	100	155	0
md_0_4_A	A	111	T	0.35568	0.96069	TRUE	0.48816	100	155	0

Figure 19: Residues with DiscoTope above the threshold of 0.35 — md-0-4A-discotope3.csv (n = 12)

Residues with DiscoTope ≥ 0.35 — md_0_5_A_discotope3.csv (n = 20)

PDB	Chain	ResID	AA	DiscoTope	Calibrated	Epitope	RSA	pLDDT	Length	AF2 flag
md_0_5_A	A	112	R	0.48284	1.82296	TRUE	0.58276	100	155	0
md_0_5_A	A	93	I	0.47997	1.80196	TRUE	0.83083	100	155	0
md_0_5_A	A	92	R	0.46760	1.71143	TRUE	0.75455	100	155	0
md_0_5_A	A	103	T	0.46001	1.65589	TRUE	0.62788	100	155	0
md_0_5_A	A	99	Q	0.45188	1.59639	TRUE	0.73454	100	155	0
md_0_5_A	A	46	R	0.44895	1.57495	TRUE	0.62748	100	155	0
md_0_5_A	A	54	P	0.43657	1.48435	TRUE	0.69158	100	155	0
md_0_5_A	A	72	Y	0.43490	1.47213	TRUE	0.48299	100	155	0
md_0_5_A	A	49	S	0.42675	1.41249	TRUE	0.30841	100	155	0
md_0_5_A	A	108	L	0.41937	1.35848	TRUE	0.78428	100	155	0
md_0_5_A	A	55	S	0.41442	1.32226	TRUE	0.28058	100	155	0
md_0_5_A	A	88	D	0.39209	1.15884	TRUE	0.52195	100	155	0
md_0_5_A	A	147	S	0.38206	1.08544	TRUE	0.54112	100	155	0
md_0_5_A	A	123	S	0.37755	1.05244	TRUE	0.47171	100	155	0
md_0_5_A	A	74	A	0.37738	1.05120	TRUE	0.85232	100	155	0
md_0_5_A	A	90	R	0.36949	0.99346	TRUE	0.50007	100	155	0
md_0_5_A	A	115	D	0.36251	0.94238	TRUE	0.44420	100	155	0
md_0_5_A	A	85	G	0.36183	0.93740	TRUE	0.50924	100	155	0
md_0_5_A	A	102	P	0.36168	0.93630	TRUE	0.96794	100	155	0
md_0_5_A	A	50	E	0.35993	0.92349	TRUE	0.56567	100	155	0

Figure 20: Residues with DiscoTope above the threshold of 0.35 — md-0-5-A-discotope3.csv (n = 20)

Residues with DiscoTope ≥ 0.35 — md_0_6_A_discotope3.csv (n = 17)

PDB	Chain	ResID	AA	DiscoTope	Calibrated	Epitope	RSA	pLDDT	Length	AF2 flag
md_0_6_A	A	54	P	0.47856	1.86845	TRUE	0.63013	100	155	0
md_0_6_A	A	21	I	0.45816	1.71276	TRUE	0.80112	100	155	0
md_0_6_A	A	146	S	0.45756	1.70818	TRUE	0.78592	100	155	0
md_0_6_A	A	111	T	0.41716	1.39985	TRUE	0.43173	100	155	0
md_0_6_A	A	64	D	0.41192	1.35986	TRUE	0.70138	100	155	0
md_0_6_A	A	99	Q	0.40949	1.34132	TRUE	0.90009	100	155	0
md_0_6_A	A	115	D	0.40204	1.28446	TRUE	0.30498	100	155	0
md_0_6_A	A	55	S	0.39292	1.21486	TRUE	0.27762	100	155	0
md_0_6_A	A	72	Y	0.39113	1.20120	TRUE	0.54704	100	155	0
md_0_6_A	A	65	S	0.39075	1.19830	TRUE	0.60540	100	155	0
md_0_6_A	A	46	R	0.38888	1.18403	TRUE	0.59187	100	155	0
md_0_6_A	A	66	D	0.38858	1.18174	TRUE	0.60124	100	155	0
md_0_6_A	A	141	R	0.36289	0.98568	TRUE	0.35925	100	155	0
md_0_6_A	A	47	Q	0.35908	0.95660	TRUE	0.36491	100	155	0
md_0_6_A	A	38	Q	0.35167	0.90005	TRUE	0.55254	100	155	0
md_0_6_A	A	112	R	0.35089	0.89409	FALSE	0.51036	100	155	0
md_0_6_A	A	93	I	0.35026	0.88929	FALSE	0.82284	100	155	0

Figure 21: Residues with DiscoTope above the threshold of 0.35 — md-0-6-A-discotope3.csv (n = 17)

HHP and low tempeterature

Residues with DiscoTope ≥ 0.35 — md_0_7_A_discotope3.csv (n = 23)

PDB	Chain	ResID	AA	DiscoTope	Calibrated	Epitope	RSA	pLDDT	Length	AF2 flag
md_0_7_A	A	92	R	0.52084	2.02543	TRUE	0.64418	100	155	0
md_0_7_A	A	55	S	0.51581	1.98994	TRUE	0.38190	100	155	0
md_0_7_A	A	50	E	0.50078	1.88391	TRUE	0.47635	100	155	0
md_0_7_A	A	54	P	0.48335	1.76095	TRUE	0.60662	100	155	0
md_0_7_A	A	93	I	0.45110	1.53343	TRUE	0.80969	100	155	0
md_0_7_A	A	46	R	0.44027	1.45703	TRUE	0.50047	100	155	0
md_0_7_A	A	103	T	0.43819	1.44236	TRUE	0.51374	100	155	0
md_0_7_A	A	123	S	0.43463	1.41724	TRUE	0.47936	100	155	0
md_0_7_A	A	65	S	0.42396	1.34197	TRUE	0.42979	100	155	0
md_0_7_A	A	81	T	0.39960	1.17012	TRUE	0.51372	100	155	0
md_0_7_A	A	106	E	0.38250	1.04948	TRUE	0.45887	100	155	0
md_0_7_A	A	100	A	0.37375	0.98775	TRUE	0.78383	100	155	0
md_0_7_A	A	72	Y	0.37345	0.98564	TRUE	0.47759	100	155	0
md_0_7_A	A	73	N	0.37113	0.96927	TRUE	0.11515	100	155	0
md_0_7_A	A	78	P	0.37031	0.96348	TRUE	0.55117	100	155	0
md_0_7_A	A	64	D	0.36916	0.95537	TRUE	0.74232	100	155	0
md_0_7_A	A	39	Q	0.35878	0.88214	FALSE	0.77288	100	155	0
md_0_7_A	A	97	E	0.35875	0.88193	FALSE	0.33216	100	155	0
md_0_7_A	A	99	Q	0.35873	0.88179	FALSE	0.85098	100	155	0
md_0_7_A	A	66	D	0.35729	0.87163	FALSE	0.73958	100	155	0
md_0_7_A	A	109	D	0.35394	0.84800	FALSE	0.52453	100	155	0
md_0_7_A	A	147	S	0.35085	0.82620	FALSE	0.50368	100	155	0
md_0_7_A	A	53	K	0.35074	0.82542	FALSE	0.62327	100	155	0

Figure 22: Residues with DiscoTope above the threshold of 0.35 — md-0-7-A-discotope3.csv (n = 23)

Residues with DiscoTope ≥ 0.35 — md_0_8_A_discotope3.csv (n = 20)

PDB	Chain	ResID	AA	DiscoTope	Calibrated	Epitope	RSA	pLDDT	Length	AF2 flag
md_0_8_A	A	92	R	0.48539	1.80218	TRUE	0.51860	100	155	0
md_0_8_A	A	54	P	0.48449	1.79573	TRUE	0.47587	100	155	0
md_0_8_A	A	64	D	0.48224	1.77962	TRUE	0.60834	100	155	0
md_0_8_A	A	103	T	0.45223	1.56471	TRUE	0.65013	100	155	0
md_0_8_A	A	93	I	0.44116	1.48543	TRUE	0.60411	100	155	0
md_0_8_A	A	72	Y	0.43917	1.47118	TRUE	0.52489	100	155	0
md_0_8_A	A	142	S	0.43360	1.43129	TRUE	0.69077	100	155	0
md_0_8_A	A	99	Q	0.43015	1.40659	TRUE	0.86055	100	155	0
md_0_8_A	A	112	R	0.42076	1.33934	TRUE	0.52080	100	155	0
md_0_8_A	A	100	A	0.41916	1.32788	TRUE	0.78550	100	155	0
md_0_8_A	A	141	R	0.39655	1.16596	TRUE	0.41878	100	155	0
md_0_8_A	A	15	S	0.38875	1.11011	TRUE	0.53449	100	155	0
md_0_8_A	A	102	P	0.37735	1.02847	TRUE	0.85309	100	155	0
md_0_8_A	A	46	R	0.37216	0.99130	TRUE	0.63383	100	155	0
md_0_8_A	A	65	S	0.37007	0.97633	TRUE	0.47786	100	155	0
md_0_8_A	A	67	F	0.36663	0.95170	TRUE	0.35241	100	155	0
md_0_8_A	A	12	F	0.36301	0.92577	TRUE	0.20035	100	155	0
md_0_8_A	A	108	L	0.35511	0.86920	FALSE	0.94120	100	155	0
md_0_8_A	A	63	P	0.35102	0.83991	FALSE	0.30816	100	155	0
md_0_8_A	A	73	N	0.35069	0.83754	FALSE	0.17021	100	155	0

Figure 23: Residues with DiscoTope above the threshold of 0.35 — md-0-8-A-discotope3.csv (n = 20)

Residues with DiscoTope ≥ 0.35 — md_0_9_A_discotope3.csv (n = 22)

PDB	Chain	ResID	AA	DiscoTope	Calibrated	Epitope	RSA	pLDDT	Length	AF2 flag
md_0_9_A	A	92	R	0.61171	2.69769	TRUE	0.63313	100	155	0
md_0_9_A	A	103	T	0.53001	2.11458	TRUE	0.46542	100	155	0
md_0_9_A	A	93	I	0.52303	2.06476	TRUE	0.69592	100	155	0
md_0_9_A	A	46	R	0.51146	1.98218	TRUE	0.64099	100	155	0
md_0_9_A	A	91	N	0.48739	1.81039	TRUE	0.24956	100	155	0
md_0_9_A	A	38	Q	0.46494	1.65015	TRUE	0.32972	100	155	0
md_0_9_A	A	15	S	0.43810	1.45859	TRUE	0.51228	100	155	0
md_0_9_A	A	108	L	0.42569	1.37002	TRUE	0.65616	100	155	0
md_0_9_A	A	102	P	0.41050	1.26160	TRUE	0.92515	100	155	0
md_0_9_A	A	99	Q	0.41018	1.25932	TRUE	0.90499	100	155	0
md_0_9_A	A	116	D	0.38808	1.10159	TRUE	0.56881	100	155	0
md_0_9_A	A	85	G	0.38438	1.07518	TRUE	0.42006	100	155	0
md_0_9_A	A	61	R	0.37291	0.99331	TRUE	0.38115	100	155	0
md_0_9_A	A	88	D	0.36888	0.96455	TRUE	0.56971	100	155	0
md_0_9_A	A	39	Q	0.36743	0.95420	TRUE	0.82230	100	155	0
md_0_9_A	A	64	D	0.36576	0.94228	TRUE	0.68628	100	155	0
md_0_9_A	A	153	T	0.36217	0.91666	TRUE	0.44634	100	155	0
md_0_9_A	A	89	T	0.36130	0.91045	TRUE	0.64323	100	155	0
md_0_9_A	A	90	R	0.36033	0.90353	TRUE	0.28051	100	155	0
md_0_9_A	A	72	Y	0.35857	0.89097	FALSE	0.47130	100	155	0
md_0_9_A	A	122	R	0.35749	0.88326	FALSE	0.28378	100	155	0
md_0_9_A	A	59	T	0.35245	0.84729	FALSE	0.56231	100	155	0

Figure 24: Residues with DiscoTope above the threshold of 0.35 — md-0-9-A-discotope3.csv (n = 22)

Residues with DiscoTope ≥ 0.35 — md_0_10_A_discotope3.csv (n = 13)

PDB	Chain	ResID	AA	DiscoTope	Calibrated	Epitope	RSA	pLDDT	Length	AF2 flag
md_0_10_A	A	91	N	0.47046	1.83359	TRUE	0.29035	100	155	0
md_0_10_A	A	11	V	0.42690	1.49618	TRUE	0.51784	100	155	0
md_0_10_A	A	15	S	0.42618	1.49061	TRUE	0.47874	100	155	0
md_0_10_A	A	93	I	0.41611	1.41261	TRUE	0.47725	100	155	0
md_0_10_A	A	102	P	0.41601	1.41183	TRUE	0.83486	100	155	0
md_0_10_A	A	108	L	0.41463	1.40114	TRUE	0.91160	100	155	0
md_0_10_A	A	54	P	0.38117	1.14197	TRUE	0.49052	100	155	0
md_0_10_A	A	103	T	0.37965	1.13020	TRUE	0.45148	100	155	0
md_0_10_A	A	65	S	0.37752	1.11370	TRUE	0.50500	100	155	0
md_0_10_A	A	116	D	0.36085	0.98458	TRUE	0.56682	100	155	0
md_0_10_A	A	7	P	0.35708	0.95538	TRUE	0.81965	100	155	0
md_0_10_A	A	72	Y	0.35297	0.92354	TRUE	0.58386	100	155	0
md_0_10_A	A	147	S	0.35208	0.91665	TRUE	0.45864	100	155	0

Figure 25: Residues with DiscoTope above the threshold of 0.35 — md-0-10-A-discotope3.csv (n = 13)

Residues with DiscoTope ≥ 0.35 — md_0_11_A_discotope3.csv (n = 20)

PDB	Chain	ResID	AA	DiscoTope	Calibrated	Epitope	RSA	pLDDT	Length	AF2 flag
md_0_11_A	A	55	S	0.48808	1.90204	TRUE	0.24249	100	155	0
md_0_11_A	A	102	P	0.48735	1.89658	TRUE	0.76541	100	155	0
md_0_11_A	A	99	Q	0.48689	1.89314	TRUE	0.86205	100	155	0
md_0_11_A	A	91	N	0.45048	1.62086	TRUE	0.15310	100	155	0
md_0_11_A	A	92	R	0.43107	1.47570	TRUE	0.59247	100	155	0
md_0_11_A	A	93	I	0.42670	1.44302	TRUE	0.21978	100	155	0
md_0_11_A	A	64	D	0.42116	1.40160	TRUE	0.71078	100	155	0
md_0_11_A	A	103	T	0.41853	1.38193	TRUE	0.41994	100	155	0
md_0_11_A	A	88	D	0.41457	1.35231	TRUE	0.60095	100	155	0
md_0_11_A	A	46	R	0.41352	1.34446	TRUE	0.65749	100	155	0
md_0_11_A	A	54	P	0.40980	1.31664	TRUE	0.51406	100	155	0
md_0_11_A	A	38	Q	0.39539	1.20888	TRUE	0.27712	100	155	0
md_0_11_A	A	90	R	0.39031	1.17089	TRUE	0.48600	100	155	0
md_0_11_A	A	98	N	0.38749	1.14980	TRUE	0.90763	100	155	0
md_0_11_A	A	96	V	0.38402	1.12385	TRUE	0.58623	100	155	0
md_0_11_A	A	72	Y	0.38069	1.09895	TRUE	0.58485	100	155	0
md_0_11_A	A	104	T	0.38042	1.09693	TRUE	0.95742	100	155	0
md_0_11_A	A	97	E	0.37165	1.03135	TRUE	0.44173	100	155	0
md_0_11_A	A	112	R	0.37012	1.01991	TRUE	0.46176	100	155	0
md_0_11_A	A	50	E	0.36791	1.00338	TRUE	0.54313	100	155	0

Figure 26: Residues with DiscoTope above the threshold of 0.35 — md-0-11-A-discotope3.csv (n = 20)

Residues with DiscoTope ≥ 0.35 — md_0_1_A_discotope3.csv (n = 17)

PDB	Chain	ResID	AA	DiscoTope	Calibrated	Epitope	RSA	pLDDT	Length	AF2 flag
md_0_1_A	A	72	Y	0.53656	2.28066	TRUE	0.42510	100	155	0
md_0_1_A	A	46	R	0.51568	2.12340	TRUE	0.59664	100	155	0
md_0_1_A	A	147	S	0.41198	1.34241	TRUE	0.49080	100	155	0
md_0_1_A	A	92	R	0.40762	1.30957	TRUE	0.63739	100	155	0
md_0_1_A	A	54	P	0.40640	1.30038	TRUE	0.47444	100	155	0
md_0_1_A	A	111	T	0.40476	1.28803	TRUE	0.51017	100	155	0
md_0_1_A	A	85	G	0.39070	1.18214	TRUE	0.57838	100	155	0
md_0_1_A	A	10	F	0.38750	1.15804	TRUE	0.62927	100	155	0
md_0_1_A	A	112	R	0.37948	1.09764	TRUE	0.46038	100	155	0
md_0_1_A	A	53	K	0.37844	1.08981	TRUE	0.59923	100	155	0
md_0_1_A	A	39	Q	0.37410	1.05712	TRUE	0.62076	100	155	0
md_0_1_A	A	64	D	0.36856	1.01540	TRUE	0.68842	100	155	0
md_0_1_A	A	15	S	0.36829	1.01336	TRUE	0.48169	100	155	0
md_0_1_A	A	6	T	0.36445	0.98444	TRUE	0.54451	100	155	0
md_0_1_A	A	123	S	0.36199	0.96592	TRUE	0.41236	100	155	0
md_0_1_A	A	14	S	0.35895	0.94302	TRUE	0.32119	100	155	0
md_0_1_A	A	21	I	0.35686	0.92728	TRUE	0.72317	100	155	0

Figure 27: Residues with DiscoTope above the threshold of 0.35 — md-0-1-A-discotope3.csv (n = 17)

Residues with DiscoTope ≥ 0.35 — md_0_2_A_discotope3.csv (n = 22)

PDB	Chain	ResID	AA	DiscoTope	Calibrated	Epitope	RSA	pLDDT	Length	AF2 flag
md_0_2_A	A	72	Y	0.48491	1.78270	TRUE	0.48138	100	155	0
md_0_2_A	A	8	S	0.47443	1.70832	TRUE	0.67595	100	155	0
md_0_2_A	A	46	R	0.44962	1.53223	TRUE	0.55449	100	155	0
md_0_2_A	A	111	T	0.44340	1.48808	TRUE	0.59339	100	155	0
md_0_2_A	A	122	R	0.44166	1.47573	TRUE	0.54198	100	155	0
md_0_2_A	A	7	P	0.43277	1.41264	TRUE	0.94366	100	155	0
md_0_2_A	A	42	T	0.42963	1.39035	TRUE	0.50326	100	155	0
md_0_2_A	A	39	Q	0.41721	1.30220	TRUE	0.88608	100	155	0
md_0_2_A	A	61	R	0.41218	1.26650	TRUE	0.47368	100	155	0
md_0_2_A	A	92	R	0.40842	1.23981	TRUE	0.50524	100	155	0
md_0_2_A	A	77	D	0.40614	1.22363	TRUE	0.25022	100	155	0
md_0_2_A	A	109	D	0.40611	1.22342	TRUE	0.34110	100	155	0
md_0_2_A	A	99	Q	0.40564	1.22008	TRUE	0.68130	100	155	0
md_0_2_A	A	147	S	0.38995	1.10872	TRUE	0.42777	100	155	0
md_0_2_A	A	112	R	0.38916	1.10312	TRUE	0.38079	100	155	0
md_0_2_A	A	32	G	0.38902	1.10212	TRUE	0.75942	100	155	0
md_0_2_A	A	10	F	0.38786	1.09389	TRUE	0.57975	100	155	0
md_0_2_A	A	5	T	0.38705	1.08814	TRUE	0.89541	100	155	0
md_0_2_A	A	6	T	0.36748	0.94924	TRUE	0.43084	100	155	0
md_0_2_A	A	64	D	0.36607	0.93923	TRUE	0.61786	100	155	0
md_0_2_A	A	85	G	0.35677	0.87323	FALSE	0.36382	100	155	0
md_0_2_A	A	93	I	0.35196	0.83909	FALSE	0.92978	100	155	0

Figure 28: Residues with DiscoTope above the threshold of 0.35 — md-0-2-A-discotope3.csv (n = 22)

Residues with DiscoTope ≥ 0.35 — md_0_3_A_discotope3.csv (n = 21)

PDB	Chain	ResID	AA	DiscoTope	Calibrated	Epitope	RSA	pLDDT	Length	AF2 flag
md_0_3_A	A	46	R	0.48956	1.80627	TRUE	0.70207	100	155	0
md_0_3_A	A	81	T	0.48560	1.77831	TRUE	0.52678	100	155	0
md_0_3_A	A	92	R	0.46407	1.62630	TRUE	0.44802	100	155	0
md_0_3_A	A	99	Q	0.45770	1.58132	TRUE	0.86250	100	155	0
md_0_3_A	A	7	P	0.45143	1.53705	TRUE	0.80081	100	155	0
md_0_3_A	A	93	I	0.44223	1.47209	TRUE	0.89269	100	155	0
md_0_3_A	A	72	Y	0.41744	1.29706	TRUE	0.44171	100	155	0
md_0_3_A	A	54	P	0.40900	1.23747	TRUE	0.54410	100	155	0
md_0_3_A	A	112	R	0.40793	1.22991	TRUE	0.65364	100	155	0
md_0_3_A	A	71	R	0.40711	1.22413	TRUE	0.23334	100	155	0
md_0_3_A	A	98	N	0.40632	1.21855	TRUE	0.27942	100	155	0
md_0_3_A	A	36	Q	0.38855	1.09308	TRUE	0.52009	100	155	0
md_0_3_A	A	119	V	0.38855	1.09308	TRUE	0.57886	100	155	0
md_0_3_A	A	115	D	0.38854	1.09301	TRUE	0.40272	100	155	0
md_0_3_A	A	152	W	0.38341	1.05679	TRUE	0.86363	100	155	0
md_0_3_A	A	52	W	0.37716	1.01266	TRUE	0.22466	100	155	0
md_0_3_A	A	58	V	0.37659	1.00863	TRUE	0.68879	100	155	0
md_0_3_A	A	100	A	0.37622	1.00602	TRUE	0.72171	100	155	0
md_0_3_A	A	97	E	0.36490	0.92610	TRUE	0.52653	100	155	0
md_0_3_A	A	151	V	0.35534	0.85860	FALSE	0.84815	100	155	0
md_0_3_A	A	49	S	0.35196	0.83473	FALSE	0.61196	100	155	0

Figure 29: Residues with DiscoTope above the threshold of 0.35 — md-0-3-A-discotope3.csv (n = 21)

Residues with DiscoTope ≥ 0.35 — md_0_4_A_discotope3.csv (n = 21)

PDB	Chain	ResID	AA	DiscoTope	Calibrated	Epitope	RSA	pLDDT	Length	AF2 flag
md_0_4_A	A	92	R	0.49669	1.88454	TRUE	0.85693	100	155	0
md_0_4_A	A	6	T	0.45693	1.59959	TRUE	0.50128	100	155	0
md_0_4_A	A	10	F	0.43211	1.42171	TRUE	0.52851	100	155	0
md_0_4_A	A	97	E	0.40556	1.23143	TRUE	0.70839	100	155	0
md_0_4_A	A	46	R	0.40359	1.21731	TRUE	0.59103	100	155	0
md_0_4_A	A	88	D	0.39822	1.17883	TRUE	0.61402	100	155	0
md_0_4_A	A	108	L	0.39504	1.15604	TRUE	0.70674	100	155	0
md_0_4_A	A	72	Y	0.39350	1.14500	TRUE	0.39599	100	155	0
md_0_4_A	A	37	T	0.39016	1.12106	TRUE	0.26308	100	155	0
md_0_4_A	A	39	Q	0.38672	1.09641	TRUE	0.66524	100	155	0
md_0_4_A	A	93	I	0.38147	1.05878	TRUE	0.88457	100	155	0
md_0_4_A	A	146	S	0.38006	1.04868	TRUE	0.61808	100	155	0
md_0_4_A	A	14	S	0.37490	1.01169	TRUE	0.37224	100	155	0
md_0_4_A	A	103	T	0.37338	1.00080	TRUE	0.79568	100	155	0
md_0_4_A	A	147	S	0.36525	0.94253	TRUE	0.59056	100	155	0
md_0_4_A	A	102	P	0.36357	0.93049	TRUE	0.85029	100	155	0
md_0_4_A	A	90	R	0.36023	0.90656	TRUE	0.31696	100	155	0
md_0_4_A	A	8	S	0.35661	0.88061	FALSE	0.54386	100	155	0
md_0_4_A	A	152	W	0.35550	0.87266	FALSE	0.75713	100	155	0
md_0_4_A	A	100	A	0.35538	0.87180	FALSE	0.69687	100	155	0
md_0_4_A	A	32	G	0.35147	0.84378	FALSE	0.52664	100	155	0

Figure 30: Residues with DiscoTope above the threshold of 0.35 — md-0-4A-discotope3.csv (n = 21)

Residues with DiscoTope ≥ 0.35 — md_0_5_A_discotope3.csv (n = 23)

PDB	Chain	ResID	AA	DiscoTope	Calibrated	Epitope	RSA	pLDDT	Length	AF2 flag
md_0_5_A	A	147	S	0.49415	1.79855	TRUE	0.49100	100	155	0
md_0_5_A	A	72	Y	0.47987	1.69992	TRUE	0.41202	100	155	0
md_0_5_A	A	123	S	0.42486	1.32000	TRUE	0.45877	100	155	0
md_0_5_A	A	10	F	0.41064	1.22179	TRUE	0.54765	100	155	0
md_0_5_A	A	112	R	0.40842	1.20645	TRUE	0.56850	100	155	0
md_0_5_A	A	29	N	0.40784	1.20245	TRUE	0.65165	100	155	0
md_0_5_A	A	102	P	0.40536	1.18532	TRUE	1.01620	100	155	0
md_0_5_A	A	5	T	0.40443	1.17890	TRUE	0.73329	100	155	0
md_0_5_A	A	46	R	0.40405	1.17627	TRUE	0.57956	100	155	0
md_0_5_A	A	32	G	0.40074	1.15341	TRUE	0.75772	100	155	0
md_0_5_A	A	11	V	0.39948	1.14471	TRUE	0.52149	100	155	0
md_0_5_A	A	146	S	0.39736	1.13007	TRUE	0.73435	100	155	0
md_0_5_A	A	7	P	0.39643	1.12364	TRUE	0.85634	100	155	0
md_0_5_A	A	85	G	0.39307	1.10044	TRUE	0.39340	100	155	0
md_0_5_A	A	88	D	0.38964	1.07675	TRUE	0.58381	100	155	0
md_0_5_A	A	8	S	0.38293	1.03041	TRUE	0.52400	100	155	0
md_0_5_A	A	50	E	0.38192	1.02343	TRUE	0.68869	100	155	0
md_0_5_A	A	6	T	0.37657	0.98648	TRUE	0.46378	100	155	0
md_0_5_A	A	156	P	0.37268	0.95961	TRUE	0.86162	100	155	0
md_0_5_A	A	92	R	0.36340	0.89552	FALSE	0.74380	100	155	0
md_0_5_A	A	126	N	0.35583	0.84324	FALSE	0.50360	100	155	0
md_0_5_A	A	99	Q	0.35399	0.83053	FALSE	0.41451	100	155	0
md_0_5_A	A	65	S	0.35253	0.82045	FALSE	0.75294	100	155	0

Figure 31: Residues with DiscoTope above the threshold of 0.35 — md-0-5-A-discotope3.csv (n = 23)

Residues with DiscoTope ≥ 0.35 — md_0_6_A_discotope3.csv (n = 29)

PDB	Chain	ResID	AA	DiscoTope	Calibrated	Epitope	RSA	pLDDT	Length	AF2 flag
md_0_6_A	A	72	Y	0.54050	2.12887	TRUE	0.45333	100	155	0
md_0_6_A	A	7	P	0.48016	1.71012	TRUE	0.81149	100	155	0
md_0_6_A	A	34	Q	0.46837	1.62830	TRUE	0.60123	100	155	0
md_0_6_A	A	99	Q	0.44671	1.47799	TRUE	0.43703	100	155	0
md_0_6_A	A	6	T	0.44561	1.47035	TRUE	0.42091	100	155	0
md_0_6_A	A	46	R	0.43820	1.41893	TRUE	0.61055	100	155	0
md_0_6_A	A	108	L	0.43529	1.39873	TRUE	0.74692	100	155	0
md_0_6_A	A	10	F	0.43403	1.38999	TRUE	0.51185	100	155	0
md_0_6_A	A	115	D	0.42921	1.35654	TRUE	0.26367	100	155	0
md_0_6_A	A	102	P	0.42473	1.32545	TRUE	0.99251	100	155	0
md_0_6_A	A	105	A	0.42376	1.31872	TRUE	0.84614	100	155	0
md_0_6_A	A	103	T	0.42223	1.30810	TRUE	0.48935	100	155	0
md_0_6_A	A	106	E	0.41807	1.27923	TRUE	0.72817	100	155	0
md_0_6_A	A	101	N	0.41676	1.27014	TRUE	0.25296	100	155	0
md_0_6_A	A	8	S	0.41378	1.24946	TRUE	0.51854	100	155	0
md_0_6_A	A	81	T	0.41070	1.22809	TRUE	0.58696	100	155	0
md_0_6_A	A	88	D	0.40832	1.21157	TRUE	0.65992	100	155	0
md_0_6_A	A	97	E	0.40784	1.20824	TRUE	0.59979	100	155	0
md_0_6_A	A	5	T	0.40576	1.19380	TRUE	0.88462	100	155	0
md_0_6_A	A	42	T	0.40092	1.16021	TRUE	0.44124	100	155	0
md_0_6_A	A	32	G	0.40023	1.15543	TRUE	0.72303	100	155	0
md_0_6_A	A	11	V	0.39180	1.09692	TRUE	0.45414	100	155	0
md_0_6_A	A	154	S	0.37677	0.99262	TRUE	0.85476	100	155	0
md_0_6_A	A	14	S	0.37271	0.96444	TRUE	0.39739	100	155	0
md_0_6_A	A	112	R	0.37034	0.94800	TRUE	0.55402	100	155	0
md_0_6_A	A	73	N	0.36948	0.94203	TRUE	0.15774	100	155	0
md_0_6_A	A	147	S	0.36100	0.88318	FALSE	0.69378	100	155	0
md_0_6_A	A	100	A	0.35780	0.86097	FALSE	0.80101	100	155	0
md_0_6_A	A	38	Q	0.35348	0.83099	FALSE	0.59419	100	155	0

Figure 32: Residues with DiscoTope above the threshold of 0.35 — md-0-6-A-discotope3.csv (n = 29)

Residues with DiscoTope ≥ 0.35 — md_0_7_A_discotope3.csv (n = 14)

PDB	Chain	ResID	AA	DiscoTope	Calibrated	Epitope	RSA	pLDDT	Length	AF2 flag
md_0_7_A	A	46	R	0.49347	1.94219	TRUE	0.60173	100	155	0
md_0_7_A	A	108	L	0.48058	1.84580	TRUE	0.90332	100	155	0
md_0_7_A	A	72	Y	0.48022	1.84311	TRUE	0.43029	100	155	0
md_0_7_A	A	104	T	0.42920	1.46160	TRUE	0.86744	100	155	0
md_0_7_A	A	93	I	0.41880	1.38384	TRUE	0.77583	100	155	0
md_0_7_A	A	7	P	0.38934	1.16354	TRUE	0.85638	100	155	0
md_0_7_A	A	103	T	0.38895	1.16063	TRUE	0.52343	100	155	0
md_0_7_A	A	85	G	0.38559	1.13550	TRUE	0.35487	100	155	0
md_0_7_A	A	50	E	0.37052	1.02282	TRUE	0.63089	100	155	0
md_0_7_A	A	92	R	0.36852	1.00786	TRUE	0.65661	100	155	0
md_0_7_A	A	90	R	0.36137	0.95439	TRUE	0.33010	100	155	0
md_0_7_A	A	8	S	0.36022	0.94580	TRUE	0.79437	100	155	0
md_0_7_A	A	102	P	0.35676	0.91992	TRUE	1.03681	100	155	0
md_0_7_A	A	116	D	0.35065	0.87423	FALSE	0.61045	100	155	0

Figure 33: Residues with DiscoTope above the threshold of 0.35 — md-0-7-A-discotope3.csv (n = 14)

Residues with DiscoTope ≥ 0.35 — md_0_8_A_discotope3.csv (n = 25)

PDB	Chain	ResID	AA	DiscoTope	Calibrated	Epitope	RSA	pLDDT	Length	AF2 flag
md_0_8_A	A	108	L	0.49513	1.81617	TRUE	0.68210	100	155	0
md_0_8_A	A	37	T	0.48560	1.74996	TRUE	0.55845	100	155	0
md_0_8_A	A	46	R	0.44960	1.49983	TRUE	0.53153	100	155	0
md_0_8_A	A	99	Q	0.44040	1.43590	TRUE	0.69718	100	155	0
md_0_8_A	A	152	W	0.43500	1.39838	TRUE	0.79094	100	155	0
md_0_8_A	A	115	D	0.42708	1.34336	TRUE	0.38813	100	155	0
md_0_8_A	A	103	T	0.42191	1.30743	TRUE	0.49764	100	155	0
md_0_8_A	A	106	E	0.41794	1.27985	TRUE	0.63167	100	155	0
md_0_8_A	A	100	A	0.41195	1.23823	TRUE	0.76979	100	155	0
md_0_8_A	A	112	R	0.41105	1.23198	TRUE	0.54239	100	155	0
md_0_8_A	A	102	P	0.40739	1.20655	TRUE	1.08217	100	155	0
md_0_8_A	A	104	T	0.40418	1.18425	TRUE	0.69481	100	155	0
md_0_8_A	A	72	Y	0.40067	1.15986	TRUE	0.43072	100	155	0
md_0_8_A	A	88	D	0.39402	1.11365	TRUE	0.70691	100	155	0
md_0_8_A	A	119	V	0.39190	1.09892	TRUE	0.47984	100	155	0
md_0_8_A	A	59	T	0.39086	1.09170	TRUE	0.89864	100	155	0
md_0_8_A	A	61	R	0.38948	1.08211	TRUE	0.35067	100	155	0
md_0_8_A	A	32	G	0.37535	0.98393	TRUE	0.77973	100	155	0
md_0_8_A	A	77	D	0.37109	0.95434	TRUE	0.29272	100	155	0
md_0_8_A	A	34	Q	0.36625	0.92071	TRUE	0.69549	100	155	0
md_0_8_A	A	122	R	0.36140	0.88701	FALSE	0.41399	100	155	0
md_0_8_A	A	153	T	0.36003	0.87749	FALSE	0.31026	100	155	0
md_0_8_A	A	126	N	0.35530	0.84463	FALSE	0.47186	100	155	0
md_0_8_A	A	42	T	0.35393	0.83511	FALSE	0.46003	100	155	0
md_0_8_A	A	5	T	0.35051	0.81134	FALSE	0.73788	100	155	0

Figure 34: Residues with DiscoTope above the threshold of 0.35 — md-0-8-A-discotope3.csv (n = 25)

Residues with DiscoTope ≥ 0.35 — md_0_9_A_discotope3.csv (n = 26)

PDB	Chain	ResID	AA	DiscoTope	Calibrated	Epitope	RSA	pLDDT	Length	AF2 flag
md_0_9_A	A	72	Y	0.50176	1.99711	TRUE	0.45068	100	155	0
md_0_9_A	A	46	R	0.48668	1.88475	TRUE	0.60805	100	155	0
md_0_9_A	A	115	D	0.45526	1.65063	TRUE	0.29201	100	155	0
md_0_9_A	A	100	A	0.44696	1.58878	TRUE	0.94406	100	155	0
md_0_9_A	A	15	S	0.43071	1.46770	TRUE	0.46928	100	155	0
md_0_9_A	A	112	R	0.42746	1.44348	TRUE	0.64573	100	155	0
md_0_9_A	A	106	E	0.42000	1.38790	TRUE	0.69877	100	155	0
md_0_9_A	A	8	S	0.41589	1.35727	TRUE	0.85347	100	155	0
md_0_9_A	A	101	N	0.40409	1.26935	TRUE	0.29287	100	155	0
md_0_9_A	A	39	Q	0.40170	1.25154	TRUE	0.74012	100	155	0
md_0_9_A	A	47	Q	0.40035	1.24148	TRUE	0.44466	100	155	0
md_0_9_A	A	102	P	0.39134	1.17434	TRUE	0.64177	100	155	0
md_0_9_A	A	103	T	0.38877	1.15519	TRUE	0.45531	100	155	0
md_0_9_A	A	34	Q	0.38806	1.14990	TRUE	0.70298	100	155	0
md_0_9_A	A	105	A	0.37538	1.05542	TRUE	0.97061	100	155	0
md_0_9_A	A	104	T	0.37529	1.05475	TRUE	0.44735	100	155	0
md_0_9_A	A	33	N	0.37231	1.03255	TRUE	0.65544	100	155	0
md_0_9_A	A	9	Q	0.37097	1.02256	TRUE	0.45763	100	155	0
md_0_9_A	A	88	D	0.36949	1.01153	TRUE	0.53607	100	155	0
md_0_9_A	A	123	S	0.36669	0.99067	TRUE	0.48912	100	155	0
md_0_9_A	A	42	T	0.36351	0.96697	TRUE	0.42422	100	155	0
md_0_9_A	A	74	A	0.36049	0.94447	TRUE	0.82183	100	155	0
md_0_9_A	A	97	E	0.36035	0.94343	TRUE	0.53501	100	155	0
md_0_9_A	A	85	G	0.35841	0.92897	TRUE	0.30716	100	155	0
md_0_9_A	A	32	G	0.35475	0.90170	TRUE	0.72157	100	155	0
md_0_9_A	A	7	P	0.35326	0.89060	FALSE	0.93472	100	155	0

Figure 35: Residues with DiscoTope above the threshold of 0.35 — md-0-9-A-discotope3.csv (n = 26)

Residues with DiscoTope ≥ 0.35 — md_0_10_A_discotope3.csv (n = 18)

PDB	Chain	ResID	AA	DiscoTope	Calibrated	Epitope	RSA	pLDDT	Length	AF2 flag
md_0_10_A	A	99	Q	0.57888	2.53298	TRUE	0.62786	100	155	0
md_0_10_A	A	46	R	0.52448	2.13374	TRUE	0.68060	100	155	0
md_0_10_A	A	102	P	0.49740	1.93500	TRUE	0.93350	100	155	0
md_0_10_A	A	72	Y	0.46418	1.69120	TRUE	0.46202	100	155	0
md_0_10_A	A	37	T	0.45640	1.63411	TRUE	0.18986	100	155	0
md_0_10_A	A	103	T	0.44234	1.53092	TRUE	0.41521	100	155	0
md_0_10_A	A	101	N	0.43048	1.44388	TRUE	0.31865	100	155	0
md_0_10_A	A	34	Q	0.43029	1.44249	TRUE	0.67257	100	155	0
md_0_10_A	A	39	Q	0.41636	1.34026	TRUE	0.70015	100	155	0
md_0_10_A	A	32	G	0.41389	1.32213	TRUE	0.78900	100	155	0
md_0_10_A	A	105	A	0.40320	1.24368	TRUE	0.73821	100	155	0
md_0_10_A	A	42	T	0.39226	1.16339	TRUE	0.42613	100	155	0
md_0_10_A	A	81	T	0.38609	1.11811	TRUE	0.54759	100	155	0
md_0_10_A	A	152	W	0.37885	1.06497	TRUE	0.74493	100	155	0
md_0_10_A	A	147	S	0.37811	1.05954	TRUE	0.48421	100	155	0
md_0_10_A	A	106	E	0.37737	1.05411	TRUE	0.70597	100	155	0
md_0_10_A	A	104	T	0.37495	1.03635	TRUE	0.50421	100	155	0
md_0_10_A	A	54	P	0.35541	0.89295	FALSE	0.76402	100	155	0

Figure 36: Residues with DiscoTope above the threshold of 0.35 — md-0-10-A-discotope3.csv (n = 18)

Residues with DiscoTope ≥ 0.35 — md_0_11_A_discotope3.csv (n = 21)

PDB	Chain	ResID	AA	DiscoTope	Calibrated	Epitope	RSA	pLDDT	Length	AF2 flag
md_0_11_A	A	72	Y	0.48959	1.90884	TRUE	0.44136	100	155	0
md_0_11_A	A	7	P	0.47847	1.82587	TRUE	0.60836	100	155	0
md_0_11_A	A	46	R	0.46495	1.72501	TRUE	0.59776	100	155	0
md_0_11_A	A	85	G	0.44066	1.54379	TRUE	0.49718	100	155	0
md_0_11_A	A	92	R	0.42637	1.43717	TRUE	0.66902	100	155	0
md_0_11_A	A	115	D	0.42595	1.43404	TRUE	0.30772	100	155	0
md_0_11_A	A	104	T	0.41304	1.33772	TRUE	0.56673	100	155	0
md_0_11_A	A	108	L	0.41129	1.32467	TRUE	0.78001	100	155	0
md_0_11_A	A	112	R	0.40998	1.31489	TRUE	0.64451	100	155	0
md_0_11_A	A	33	N	0.40709	1.29333	TRUE	0.67487	100	155	0
md_0_11_A	A	106	E	0.38987	1.16486	TRUE	0.75449	100	155	0
md_0_11_A	A	102	P	0.38876	1.15658	TRUE	0.95539	100	155	0
md_0_11_A	A	119	V	0.37599	1.06130	TRUE	0.53316	100	155	0
md_0_11_A	A	50	E	0.37269	1.03668	TRUE	0.56288	100	155	0
md_0_11_A	A	105	A	0.37204	1.03183	TRUE	0.69187	100	155	0
md_0_11_A	A	99	Q	0.37080	1.02258	TRUE	0.48551	100	155	0
md_0_11_A	A	81	T	0.36814	1.00274	TRUE	0.53147	100	155	0
md_0_11_A	A	77	D	0.36776	0.99990	TRUE	0.32878	100	155	0
md_0_11_A	A	54	P	0.36550	0.98304	TRUE	0.49838	100	155	0
md_0_11_A	A	39	Q	0.36538	0.98215	TRUE	0.48604	100	155	0
md_0_11_A	A	32	G	0.36124	0.95126	TRUE	0.74303	100	155	0

Figure 37: Residues with DiscoTope above the threshold of 0.35 — md-0-11-A-discotope3.csv (n = 21)

Residues with DiscoTope ≥ 0.35 — md_0_12_A_discotope3.csv (n = 22)

PDB	Chain	ResID	AA	DiscoTope	Calibrated	Epitope	RSA	pLDDT	Length	AF2 flag
md_0_12_A	A	72	Y	0.50460	1.96551	TRUE	0.41458	100	155	0
md_0_12_A	A	108	L	0.49198	1.87394	TRUE	0.93495	100	155	0
md_0_12_A	A	46	R	0.47366	1.74100	TRUE	0.59982	100	155	0
md_0_12_A	A	99	Q	0.45789	1.62656	TRUE	0.58769	100	155	0
md_0_12_A	A	85	G	0.45206	1.58426	TRUE	0.48139	100	155	0
md_0_12_A	A	106	E	0.44412	1.52664	TRUE	0.73658	100	155	0
md_0_12_A	A	93	I	0.43197	1.43848	TRUE	0.72536	100	155	0
md_0_12_A	A	112	R	0.42779	1.40814	TRUE	0.65439	100	155	0
md_0_12_A	A	90	R	0.42751	1.40611	TRUE	0.64557	100	155	0
md_0_12_A	A	37	T	0.42184	1.36497	TRUE	0.15868	100	155	0
md_0_12_A	A	92	R	0.42094	1.35844	TRUE	0.39213	100	155	0
md_0_12_A	A	42	T	0.41451	1.31178	TRUE	0.58256	100	155	0
md_0_12_A	A	116	D	0.40725	1.25910	TRUE	0.62777	100	155	0
md_0_12_A	A	39	Q	0.40219	1.22238	TRUE	0.64046	100	155	0
md_0_12_A	A	59	T	0.39193	1.14793	TRUE	0.58207	100	155	0
md_0_12_A	A	152	W	0.38992	1.13334	TRUE	0.78244	100	155	0
md_0_12_A	A	103	T	0.38863	1.12398	TRUE	0.42472	100	155	0
md_0_12_A	A	96	V	0.38595	1.10453	TRUE	0.58992	100	155	0
md_0_12_A	A	107	T	0.38506	1.09807	TRUE	0.36103	100	155	0
md_0_12_A	A	8	S	0.38233	1.07826	TRUE	0.73085	100	155	0
md_0_12_A	A	77	D	0.37423	1.01949	TRUE	0.27241	100	155	0
md_0_12_A	A	105	A	0.36041	0.91920	TRUE	0.58861	100	155	0

Figure 38: Residues with DiscoTope above the threshold of 0.35 — md-0-12-A-discotope3.csv (n = 22)

Residues with DiscoTope ≥ 0.35 — md_0_13_A_discotope3.csv (n = 24)

PDB	Chain	ResID	AA	DiscoTope	Calibrated	Epitope	RSA	pLDDT	Length	AF2 flag
md_0_13_A	A	108	L	0.51922	1.98066	TRUE	0.48027	100	155	0
md_0_13_A	A	46	R	0.51656	1.96220	TRUE	0.63070	100	155	0
md_0_13_A	A	109	D	0.48906	1.77141	TRUE	0.63210	100	155	0
md_0_13_A	A	102	P	0.48171	1.72042	TRUE	0.94261	100	155	0
md_0_13_A	A	101	N	0.47845	1.69780	TRUE	0.38150	100	155	0
md_0_13_A	A	103	T	0.45420	1.52955	TRUE	0.35940	100	155	0
md_0_13_A	A	100	A	0.44370	1.45671	TRUE	0.96003	100	155	0
md_0_13_A	A	106	E	0.44272	1.44991	TRUE	0.66730	100	155	0
md_0_13_A	A	43	V	0.43469	1.39420	TRUE	0.57149	100	155	0
md_0_13_A	A	54	P	0.43202	1.37567	TRUE	0.63063	100	155	0
md_0_13_A	A	98	N	0.41869	1.28319	TRUE	0.35494	100	155	0
md_0_13_A	A	123	S	0.41853	1.28208	TRUE	0.43790	100	155	0
md_0_13_A	A	96	V	0.41337	1.24628	TRUE	0.46625	100	155	0
md_0_13_A	A	92	R	0.40860	1.21319	TRUE	0.35258	100	155	0
md_0_13_A	A	112	R	0.40207	1.16788	TRUE	0.57715	100	155	0
md_0_13_A	A	152	W	0.39454	1.11564	TRUE	0.80740	100	155	0
md_0_13_A	A	97	E	0.37872	1.00588	TRUE	0.72887	100	155	0
md_0_13_A	A	99	Q	0.37223	0.96085	TRUE	0.51660	100	155	0
md_0_13_A	A	72	Y	0.37014	0.94635	TRUE	0.45012	100	155	0
md_0_13_A	A	119	V	0.36817	0.93269	TRUE	0.55806	100	155	0
md_0_13_A	A	5	T	0.36087	0.88204	FALSE	0.82467	100	155	0
md_0_13_A	A	8	S	0.35606	0.84867	FALSE	0.65636	100	155	0
md_0_13_A	A	85	G	0.35274	0.82563	FALSE	0.55755	100	155	0
md_0_13_A	A	126	N	0.35004	0.80690	FALSE	0.54976	100	155	0

Figure 39: Residues with DiscoTope above the threshold of 0.35 — md-0-13-A-discotope3.csv (n = 24)

Residues with DiscoTope ≥ 0.35 — md_0_14_A_discotope3.csv (n = 29)

PDB	Chain	ResID	AA	DiscoTope	Calibrated	Epitope	RSA	pLDDT	Length	AF2 flag
md_0_14_A	A	99	Q	0.54888	2.15519	TRUE	0.69417	100	155	0
md_0_14_A	A	106	E	0.52800	2.01240	TRUE	0.60579	100	155	0
md_0_14_A	A	107	T	0.51204	1.90325	TRUE	0.36621	100	155	0
md_0_14_A	A	112	R	0.50750	1.87221	TRUE	0.53505	100	155	0
md_0_14_A	A	109	D	0.46489	1.58081	TRUE	0.60716	100	155	0
md_0_14_A	A	39	Q	0.45743	1.52979	TRUE	0.68431	100	155	0
md_0_14_A	A	103	T	0.45685	1.52582	TRUE	0.32263	100	155	0
md_0_14_A	A	108	L	0.45149	1.48917	TRUE	0.39890	100	155	0
md_0_14_A	A	102	P	0.45114	1.48677	TRUE	0.90699	100	155	0
md_0_14_A	A	119	V	0.44188	1.42345	TRUE	0.53588	100	155	0
md_0_14_A	A	72	Y	0.42960	1.33947	TRUE	0.49797	100	155	0
md_0_14_A	A	152	W	0.42794	1.32811	TRUE	0.75698	100	155	0
md_0_14_A	A	100	A	0.42312	1.29515	TRUE	0.95136	100	155	0
md_0_14_A	A	29	N	0.41293	1.22546	TRUE	0.38180	100	155	0
md_0_14_A	A	98	N	0.40804	1.19202	TRUE	0.27278	100	155	0
md_0_14_A	A	32	G	0.40488	1.17041	TRUE	0.74080	100	155	0
md_0_14_A	A	101	N	0.40203	1.15092	TRUE	0.37067	100	155	0
md_0_14_A	A	43	V	0.39547	1.10606	TRUE	0.37748	100	155	0
md_0_14_A	A	97	E	0.38985	1.06762	TRUE	0.61707	100	155	0
md_0_14_A	A	115	D	0.38925	1.06352	TRUE	0.19195	100	155	0
md_0_14_A	A	34	Q	0.38518	1.03569	TRUE	0.31886	100	155	0
md_0_14_A	A	33	N	0.37744	0.98275	TRUE	0.53687	100	155	0
md_0_14_A	A	105	A	0.37292	0.95184	TRUE	0.87185	100	155	0
md_0_14_A	A	81	T	0.36505	0.89802	FALSE	0.51947	100	155	0
md_0_14_A	A	74	A	0.36466	0.89536	FALSE	0.80788	100	155	0
md_0_14_A	A	47	Q	0.36013	0.86438	FALSE	0.37792	100	155	0
md_0_14_A	A	46	R	0.35668	0.84078	FALSE	0.53624	100	155	0
md_0_14_A	A	73	N	0.35107	0.80242	FALSE	0.11299	100	155	0
md_0_14_A	A	58	V	0.35094	0.80153	FALSE	0.42653	100	155	0

Figure 40: Residues with DiscoTope above the threshold of 0.35 — md-0-14-A-discotope3.csv (n = 29)

Residues with DiscoTope ≥ 0.35 — md_0_15_A_discotope3.csv (n = 34)

PDB	Chain	ResID	AA	DiscoTope	Calibrated	Epitope	RSA	pLDDT	Length	AF2 flag
md_0_15_A	A	92	R	0.52334	1.95572	TRUE	0.43520	100	155	0
md_0_15_A	A	102	P	0.51824	1.92128	TRUE	0.97367	100	155	0
md_0_15_A	A	46	R	0.50707	1.84585	TRUE	0.60616	100	155	0
md_0_15_A	A	99	Q	0.48915	1.72483	TRUE	0.73087	100	155	0
md_0_15_A	A	98	N	0.47925	1.65798	TRUE	0.30342	100	155	0
md_0_15_A	A	72	Y	0.47043	1.59841	TRUE	0.50650	100	155	0
md_0_15_A	A	107	T	0.46883	1.58761	TRUE	0.30379	100	155	0
md_0_15_A	A	109	D	0.46364	1.55256	TRUE	0.66586	100	155	0
md_0_15_A	A	49	S	0.45910	1.52190	TRUE	0.32088	100	155	0
md_0_15_A	A	100	A	0.45099	1.46713	TRUE	0.89679	100	155	0
md_0_15_A	A	96	V	0.44640	1.43614	TRUE	0.48196	100	155	0
md_0_15_A	A	90	R	0.44465	1.42432	TRUE	0.88336	100	155	0
md_0_15_A	A	97	E	0.43837	1.38191	TRUE	0.63009	100	155	0
md_0_15_A	A	106	E	0.43489	1.35841	TRUE	0.63092	100	155	0
md_0_15_A	A	93	I	0.42716	1.30621	TRUE	0.63917	100	155	0
md_0_15_A	A	39	Q	0.42154	1.26825	TRUE	0.60239	100	155	0
md_0_15_A	A	101	N	0.41965	1.25549	TRUE	0.37146	100	155	0
md_0_15_A	A	108	L	0.41811	1.24509	TRUE	0.53823	100	155	0
md_0_15_A	A	103	T	0.41683	1.23645	TRUE	0.41058	100	155	0
md_0_15_A	A	32	G	0.41173	1.20201	TRUE	0.85451	100	155	0
md_0_15_A	A	50	E	0.39846	1.11239	TRUE	0.50997	100	155	0
md_0_15_A	A	113	R	0.39397	1.08207	TRUE	0.46700	100	155	0
md_0_15_A	A	91	N	0.38742	1.03784	TRUE	0.48092	100	155	0
md_0_15_A	A	152	W	0.37840	0.97693	TRUE	0.69775	100	155	0
md_0_15_A	A	29	N	0.37424	0.94883	TRUE	0.57609	100	155	0
md_0_15_A	A	38	Q	0.36889	0.91270	TRUE	0.36737	100	155	0
md_0_15_A	A	85	G	0.36875	0.91176	TRUE	0.66018	100	155	0
md_0_15_A	A	123	S	0.36631	0.89528	FALSE	0.39675	100	155	0
md_0_15_A	A	116	D	0.35975	0.85098	FALSE	0.64473	100	155	0
md_0_15_A	A	73	N	0.35774	0.83741	FALSE	0.15295	100	155	0
md_0_15_A	A	43	V	0.35420	0.81350	FALSE	0.58076	100	155	0
md_0_15_A	A	105	A	0.35078	0.79040	FALSE	0.52897	100	155	0
md_0_15_A	A	33	N	0.35064	0.78946	FALSE	0.43323	100	155	0
md_0_15_A	A	42	T	0.35056	0.78892	FALSE	0.44201	100	155	0

Figure 41: Residues with DiscoTope above the threshold of 0.35 — md-0-15-A-discotope3.csv (n = 34)

Residues with DiscoTope ≥ 0.35 — md_0_16_A_discotope3.csv (n = 29)

PDB	Chain	ResID	AA	DiscoTope	Calibrated	Epitope	RSA	pLDDT	Length	AF2 flag
md_0_16_A	A	107	T	0.54202	2.14708	TRUE	0.30152	100	155	0
md_0_16_A	A	39	Q	0.51066	1.92867	TRUE	0.45822	100	155	0
md_0_16_A	A	93	I	0.49231	1.80087	TRUE	0.66438	100	155	0
md_0_16_A	A	109	D	0.47692	1.69368	TRUE	0.68425	100	155	0
md_0_16_A	A	108	L	0.47642	1.69020	TRUE	0.38915	100	155	0
md_0_16_A	A	72	Y	0.47454	1.67711	TRUE	0.45599	100	155	0
md_0_16_A	A	101	N	0.46191	1.58915	TRUE	0.40677	100	155	0
md_0_16_A	A	46	R	0.45995	1.57549	TRUE	0.61299	100	155	0
md_0_16_A	A	98	N	0.45353	1.53078	TRUE	0.36326	100	155	0
md_0_16_A	A	102	P	0.45332	1.52932	TRUE	0.73315	100	155	0
md_0_16_A	A	85	G	0.42460	1.32929	TRUE	0.52019	100	155	0
md_0_16_A	A	100	A	0.42290	1.31745	TRUE	1.01795	100	155	0
md_0_16_A	A	106	E	0.41578	1.26787	TRUE	0.67826	100	155	0
md_0_16_A	A	92	R	0.40496	1.19251	TRUE	0.37397	100	155	0
md_0_16_A	A	96	V	0.39778	1.14250	TRUE	0.57131	100	155	0
md_0_16_A	A	90	R	0.39624	1.13178	TRUE	0.94817	100	155	0
md_0_16_A	A	38	Q	0.39557	1.12711	TRUE	0.45236	100	155	0
md_0_16_A	A	103	T	0.39495	1.12279	TRUE	0.48553	100	155	0
md_0_16_A	A	91	N	0.39430	1.11827	TRUE	0.43032	100	155	0
md_0_16_A	A	6	T	0.39196	1.10197	TRUE	0.48543	100	155	0
md_0_16_A	A	97	E	0.38745	1.07056	TRUE	0.73848	100	155	0
md_0_16_A	A	99	Q	0.37900	1.01171	TRUE	0.50416	100	155	0
md_0_16_A	A	105	A	0.37798	1.00460	TRUE	0.36455	100	155	0
md_0_16_A	A	32	G	0.37397	0.97667	TRUE	0.76935	100	155	0
md_0_16_A	A	81	T	0.37169	0.96080	TRUE	0.50441	100	155	0
md_0_16_A	A	42	T	0.37129	0.95801	TRUE	0.50067	100	155	0
md_0_16_A	A	5	T	0.36616	0.92228	TRUE	0.86982	100	155	0
md_0_16_A	A	113	R	0.36264	0.89776	FALSE	0.52963	100	155	0
md_0_16_A	A	115	D	0.35673	0.85660	FALSE	0.16669	100	155	0

Figure 42: Residues with DiscoTope above the threshold of 0.35 — md-0-16-A-discotope3.csv (n = 29)

Residues with DiscoTope ≥ 0.35 — md_0_17_A_discotope3.csv (n = 28)

PDB	Chain	ResID	AA	DiscoTope	Calibrated	Epitope	RSA	pLDDT	Length	AF2 flag
md_0_17_A	A	72	Y	0.52861	2.07112	TRUE	0.43410	100	155	0
md_0_17_A	A	112	R	0.51382	1.96724	TRUE	0.57870	100	155	0
md_0_17_A	A	46	R	0.50072	1.87523	TRUE	0.58528	100	155	0
md_0_17_A	A	92	R	0.49598	1.84194	TRUE	0.39533	100	155	0
md_0_17_A	A	147	S	0.47622	1.70315	TRUE	0.37514	100	155	0
md_0_17_A	A	73	N	0.44076	1.45409	TRUE	0.28150	100	155	0
md_0_17_A	A	152	W	0.44043	1.45177	TRUE	0.73749	100	155	0
md_0_17_A	A	99	Q	0.43279	1.39811	TRUE	0.50761	100	155	0
md_0_17_A	A	85	G	0.42980	1.37711	TRUE	0.73842	100	155	0
md_0_17_A	A	90	R	0.42509	1.34402	TRUE	0.78013	100	155	0
md_0_17_A	A	113	R	0.42030	1.31038	TRUE	0.48061	100	155	0
md_0_17_A	A	49	S	0.41663	1.28460	TRUE	0.35056	100	155	0
md_0_17_A	A	39	Q	0.41008	1.23860	TRUE	0.66831	100	155	0
md_0_17_A	A	91	N	0.40831	1.22616	TRUE	0.51141	100	155	0
md_0_17_A	A	81	T	0.40793	1.22349	TRUE	0.50745	100	155	0
md_0_17_A	A	101	N	0.40605	1.21029	TRUE	0.29331	100	155	0
md_0_17_A	A	32	G	0.40593	1.20945	TRUE	0.73092	100	155	0
md_0_17_A	A	97	E	0.40236	1.18437	TRUE	0.66159	100	155	0
md_0_17_A	A	109	D	0.40063	1.17222	TRUE	0.77406	100	155	0
md_0_17_A	A	108	L	0.38655	1.07333	TRUE	0.36301	100	155	0
md_0_17_A	A	100	A	0.38475	1.06068	TRUE	0.99902	100	155	0
md_0_17_A	A	102	P	0.37415	0.98623	TRUE	0.97038	100	155	0
md_0_17_A	A	98	N	0.36926	0.95189	TRUE	0.37123	100	155	0
md_0_17_A	A	103	T	0.36359	0.91206	TRUE	0.39713	100	155	0
md_0_17_A	A	116	D	0.35828	0.87476	FALSE	0.65137	100	155	0
md_0_17_A	A	93	I	0.35504	0.85201	FALSE	0.62776	100	155	0
md_0_17_A	A	42	T	0.35469	0.84955	FALSE	0.40389	100	155	0
md_0_17_A	A	126	N	0.35173	0.82876	FALSE	0.54947	100	155	0

Figure 43: Residues with DiscoTope above the threshold of 0.35 — md-0-17-A-discotope3.csv (n = 28)

Residues with DiscoTope ≥ 0.35 — md_0_18_A_discotope3.csv (n = 28)

PDB	Chain	ResID	AA	DiscoTope	Calibrated	Epitope	RSA	pLDDT	Length	AF2 flag
md_0_18_A	A	123	S	0.53197	1.98516	TRUE	0.46449	100	155	0
md_0_18_A	A	99	Q	0.52575	1.94375	TRUE	0.41606	100	155	0
md_0_18_A	A	72	Y	0.52180	1.91746	TRUE	0.41053	100	155	0
md_0_18_A	A	98	N	0.48458	1.66971	TRUE	0.41686	100	155	0
md_0_18_A	A	101	N	0.47471	1.60401	TRUE	0.40062	100	155	0
md_0_18_A	A	100	A	0.47280	1.59130	TRUE	1.01161	100	155	0
md_0_18_A	A	103	T	0.46910	1.56667	TRUE	0.41340	100	155	0
md_0_18_A	A	109	D	0.46202	1.51954	TRUE	0.58869	100	155	0
md_0_18_A	A	96	V	0.45158	1.45005	TRUE	0.65197	100	155	0
md_0_18_A	A	102	P	0.45152	1.44965	TRUE	0.90625	100	155	0
md_0_18_A	A	46	R	0.42121	1.24790	TRUE	0.56293	100	155	0
md_0_18_A	A	143	S	0.41606	1.21361	TRUE	0.39115	100	155	0
md_0_18_A	A	113	R	0.40096	1.11310	TRUE	0.49473	100	155	0
md_0_18_A	A	106	E	0.39337	1.06258	TRUE	0.67414	100	155	0
md_0_18_A	A	119	V	0.39106	1.04721	TRUE	0.55402	100	155	0
md_0_18_A	A	107	T	0.38741	1.02291	TRUE	0.32095	100	155	0
md_0_18_A	A	152	W	0.38654	1.01712	TRUE	0.71380	100	155	0
md_0_18_A	A	50	E	0.38422	1.00168	TRUE	0.57075	100	155	0
md_0_18_A	A	54	P	0.38318	0.99475	TRUE	0.62407	100	155	0
md_0_18_A	A	91	N	0.37945	0.96992	TRUE	0.46602	100	155	0
md_0_18_A	A	90	R	0.37576	0.94536	TRUE	0.73206	100	155	0
md_0_18_A	A	47	Q	0.36941	0.90309	TRUE	0.48091	100	155	0
md_0_18_A	A	29	N	0.36477	0.87221	FALSE	0.54323	100	155	0
md_0_18_A	A	105	A	0.35667	0.81829	FALSE	0.47087	100	155	0
md_0_18_A	A	92	R	0.35559	0.81110	FALSE	0.37161	100	155	0
md_0_18_A	A	39	Q	0.35558	0.81104	FALSE	0.52740	100	155	0
md_0_18_A	A	93	I	0.35168	0.78508	FALSE	0.66389	100	155	0
md_0_18_A	A	97	E	0.35046	0.77696	FALSE	0.63083	100	155	0

Figure 44: Residues with DiscoTope above the threshold of 0.35 — md-0-18-A-discotope3.csv (n = 28)

Residues with DiscoTope ≥ 0.35 — md_0_19_A_discotope3.csv (n = 23)

PDB	Chain	ResID	AA	DiscoTope	Calibrated	Epitope	RSA	pLDDT	Length	AF2 flag
md_0_19_A	A	72	Y	0.49238	1.91558	TRUE	0.44788	100	155	0
md_0_19_A	A	106	E	0.46074	1.68124	TRUE	0.66735	100	155	0
md_0_19_A	A	100	A	0.45621	1.64769	TRUE	1.06917	100	155	0
md_0_19_A	A	101	N	0.44595	1.57170	TRUE	0.45503	100	155	0
md_0_19_A	A	107	T	0.44352	1.55371	TRUE	0.30134	100	155	0
md_0_19_A	A	46	R	0.43252	1.47224	TRUE	0.56871	100	155	0
md_0_19_A	A	73	N	0.41742	1.36040	TRUE	0.15379	100	155	0
md_0_19_A	A	98	N	0.41209	1.32093	TRUE	0.31501	100	155	0
md_0_19_A	A	96	V	0.41147	1.31634	TRUE	0.57559	100	155	0
md_0_19_A	A	99	Q	0.39614	1.20280	TRUE	0.39373	100	155	0
md_0_19_A	A	81	T	0.39250	1.17584	TRUE	0.48697	100	155	0
md_0_19_A	A	103	T	0.38939	1.15281	TRUE	0.44044	100	155	0
md_0_19_A	A	43	V	0.38507	1.12081	TRUE	0.57402	100	155	0
md_0_19_A	A	49	S	0.38460	1.11733	TRUE	0.30125	100	155	0
md_0_19_A	A	113	R	0.38289	1.10467	TRUE	0.54951	100	155	0
md_0_19_A	A	109	D	0.37464	1.04356	TRUE	0.63947	100	155	0
md_0_19_A	A	85	G	0.36763	0.99165	TRUE	0.62298	100	155	0
md_0_19_A	A	102	P	0.36634	0.98209	TRUE	0.93547	100	155	0
md_0_19_A	A	112	R	0.35986	0.93410	TRUE	0.55682	100	155	0
md_0_19_A	A	119	V	0.35888	0.92684	TRUE	0.54678	100	155	0
md_0_19_A	A	32	G	0.35676	0.91114	TRUE	0.85049	100	155	0
md_0_19_A	A	42	T	0.35607	0.90603	TRUE	0.51818	100	155	0
md_0_19_A	A	78	P	0.35526	0.90003	TRUE	0.52605	100	155	0

Figure 45: Residues with DiscoTope above the threshold of 0.35 — md-0-19-A-discotope3.csv (n = 23)

Residues with DiscoTope ≥ 0.35 — md_0_20_A_discotope3.csv (n = 31)

PDB	Chain	ResID	AA	DiscoTope	Calibrated	Epitope	RSA	pLDDT	Length	AF2 flag
md_0_20_A	A	46	R	0.49601	1.81831	TRUE	0.55440	100	155	0
md_0_20_A	A	93	I	0.48011	1.70808	TRUE	0.64051	100	155	0
md_0_20_A	A	90	R	0.47386	1.66475	TRUE	0.73215	100	155	0
md_0_20_A	A	106	E	0.46975	1.63625	TRUE	0.72079	100	155	0
md_0_20_A	A	92	R	0.46762	1.62149	TRUE	0.42802	100	155	0
md_0_20_A	A	102	P	0.46406	1.59681	TRUE	0.95918	100	155	0
md_0_20_A	A	100	A	0.45898	1.56159	TRUE	0.93031	100	155	0
md_0_20_A	A	99	Q	0.45487	1.53309	TRUE	0.72378	100	155	0
md_0_20_A	A	91	N	0.44650	1.47506	TRUE	0.43035	100	155	0
md_0_20_A	A	96	V	0.44577	1.47000	TRUE	0.49090	100	155	0
md_0_20_A	A	152	W	0.43838	1.41877	TRUE	0.71920	100	155	0
md_0_20_A	A	112	R	0.42444	1.32212	TRUE	0.58852	100	155	0
md_0_20_A	A	103	T	0.42237	1.30777	TRUE	0.46383	100	155	0
md_0_20_A	A	109	D	0.42110	1.29897	TRUE	0.70228	100	155	0
md_0_20_A	A	116	D	0.41987	1.29044	TRUE	0.66631	100	155	0
md_0_20_A	A	101	N	0.41049	1.22541	TRUE	0.36467	100	155	0
md_0_20_A	A	107	T	0.40820	1.20953	TRUE	0.31600	100	155	0
md_0_20_A	A	32	G	0.40734	1.20357	TRUE	0.70219	100	155	0
md_0_20_A	A	6	T	0.40587	1.19338	TRUE	0.46444	100	155	0
md_0_20_A	A	39	Q	0.40492	1.18679	TRUE	0.52782	100	155	0
md_0_20_A	A	43	V	0.39455	1.11490	TRUE	0.52714	100	155	0
md_0_20_A	A	98	N	0.38279	1.03337	TRUE	0.40247	100	155	0
md_0_20_A	A	73	N	0.38247	1.03115	TRUE	0.21553	100	155	0
md_0_20_A	A	38	Q	0.37733	0.99552	TRUE	0.38930	100	155	0
md_0_20_A	A	105	A	0.37164	0.95607	TRUE	0.45887	100	155	0
md_0_20_A	A	72	Y	0.37079	0.95017	TRUE	0.44124	100	155	0
md_0_20_A	A	97	E	0.36524	0.91170	TRUE	0.62185	100	155	0
md_0_20_A	A	108	L	0.36497	0.90983	TRUE	0.30963	100	155	0
md_0_20_A	A	119	V	0.36086	0.88133	FALSE	0.55336	100	155	0
md_0_20_A	A	33	N	0.35911	0.86920	FALSE	0.34884	100	155	0
md_0_20_A	A	115	D	0.35338	0.82947	FALSE	0.12017	100	155	0

Figure 46: Residues with DiscoTope above the threshold of 0.35 — md-0-20-A-discotope3.csv (n = 31)

Residues with DiscoTope ≥ 0.35 — md_0_21_A_discotope3.csv (n = 17)

PDB	Chain	ResID	AA	DiscoTope	Calibrated	Epitope	RSA	pLDDT	Length	AF2 flag
md_0_21_A	A	72	Y	0.48804	1.91082	TRUE	0.51879	100	155	0
md_0_21_A	A	100	A	0.47417	1.80660	TRUE	0.98278	100	155	0
md_0_21_A	A	109	D	0.47237	1.79308	TRUE	0.65815	100	155	0
md_0_21_A	A	108	L	0.46049	1.70381	TRUE	0.41812	100	155	0
md_0_21_A	A	103	T	0.45138	1.63536	TRUE	0.39768	100	155	0
md_0_21_A	A	106	E	0.43629	1.52197	TRUE	0.71179	100	155	0
md_0_21_A	A	46	R	0.43577	1.51806	TRUE	0.70497	100	155	0
md_0_21_A	A	50	E	0.42852	1.46359	TRUE	0.67623	100	155	0
md_0_21_A	A	85	G	0.41078	1.33029	TRUE	0.79369	100	155	0
md_0_21_A	A	101	N	0.40102	1.25696	TRUE	0.33843	100	155	0
md_0_21_A	A	98	N	0.37439	1.05686	TRUE	0.22547	100	155	0
md_0_21_A	A	15	S	0.35940	0.94423	TRUE	0.48513	100	155	0
md_0_21_A	A	33	N	0.35833	0.93619	TRUE	0.42157	100	155	0
md_0_21_A	A	112	R	0.35335	0.89877	FALSE	0.56220	100	155	0
md_0_21_A	A	54	P	0.35277	0.89441	FALSE	0.83967	100	155	0
md_0_21_A	A	152	W	0.35261	0.89321	FALSE	0.74441	100	155	0
md_0_21_A	A	29	N	0.35034	0.87615	FALSE	0.38198	100	155	0

Figure 47: Residues with DiscoTope above the threshold of 0.35 — md-0-21-A-discotope3.csv (n = 17)